Integrated analysis of the physiology, RNA, and microRNA involved in black locust (Robinia pseudoacacia) rejuvenation

Zijie Zhang
Beijing Forestry University
Yuhan Sun
Beijing Forestry University
Chao Han
Beijing Forestry University
Li Dong
Beijing Forestry University
Qi Guo
Beijing Forestry University
Xiuyu Li
Beijing Forestry University
Sen Cao
Beijing Forestry University
Saleem Ud Din
Beijing Forestry University
Zeeshan Munir
Beijing Forestry University
José Manuel Pérez-Pérez
Universidad Miguel Hernandez de Elche
Yun Li (yunli@bjfu.edu.cn)

Research article

Keywords: Rejuvenation, Robinia pseudoacacia, Physiological, Transcriptome, MiRNAs

Posted Date: June 19th, 2019

DOI: https://doi.org/10.21203/rs.2.10375/v1

Abstract

Background Rejuvenation is a key process that enables perennial woody plants to regain growth potential. In Robinia pseudoacacia plantations, natural root sprouting individuals provide good material for studying the rejuvenation of woody plants. However, the physiological differences and molecular mechanisms underlying black locust rejuvenation remain unclear. In this study, we compared the physiological conditions and molecular responses of rejuvenated individuals and mother trees. Results Our analysis of leaf structures and physiological indices showed that the epidermis thickness, leaf thickness and leaf-tissue tightness of rejuvenated individuals were less than those of mother trees. The soluble-sugar content and total SOD activity of rejuvenated individuals were also lower than those of mother trees. The younger the rejuvenated individuals were, the lower the ABA content, ABA/ZT and GA3/ZT in the leaves. The ZT content increased with decreasing age of rejuvenated individuals. Using high-throughput sequencing strategies, the mRNA and miRNA involved in the rejuvenation of black locust were identified. RNA-seq identified 175,862 unigenes by de novo transcript assembly. Of those, 4,727 differentially expressed genes were identified based on clean reads mapped to the assembled transcriptome for gene expression analysis(fold change≥2 or ≤0.5 and q-value≤0.05). These genes were enriched to 53 gene ontology(GO) terms and 20 KEGG pathways (FDR≤0.01). Among these were a major pathway related to flavone and flavonol biosynthesis. High-throughput miRNA sequencing identified a total of 991 miRNAs, including 671 novel miRNAs. Furthermore, 262 known and 625 novel differentially expressed miRNAs were identified(fold change≥1.5 or ≤0.67 and p≤0.05). The main functions identified in the GO analysis of the target predictions overlapped with differentially expressed genes derived from RNA-seq. KEGG pathway enrichment showed that circadian rhythm-fly and signaling pathways regulating pluripotency of stem cells attracted considerable attention during rejuvenation. Conclusion Our study revealed physiological differences between rejuvenated individuals and mother trees of R. pseudoacacia. Differential genes between mother trees and rejuvenated individuals may vary according to the tree ages, but miRNAs may play a key regulatory role in rejuvenation. The same genotype system composed of root germinating individuals and mother-tree individuals provides a solid starting point for further elucidation of the rejuvenation of woody plants.

Background

In perennial plants, a vegetative phase change usually occurs once in a life cycle, but this process can be reversible under certain circumstances. This process is defined as rejuvenation[1, 2]. Phase reversal has been observed and studied in many plants, such as wild cherry[3], *Sequoia sempervirens*[4]and *Tectona Grandis*[5]. Phase reversal can be achieved by artificial methods. Somatic embryogenesis can cause rejuvenation in mature *Quercus robur*[6]. Huang *et al.* reported that, after five instances of repeated grafting of adult shoot tips onto juvenile rootstock *in vitro*, a rejuvenation phenomenon occurred in *S. sempervirens*[4]. In *Malus xiaojinensis*, after 15 passages of in vitro subculture , micro-shoots from adult phase explants were successfully rejuvenated [7]. In addition to artificial methods for phase reversal, some natural factors can drive plant rejuvenation, such as in *Pinus sylvestris* L[8]. Morphological and

physiological restoration of rejuvenated plants have been observed. After reversed senescence of soybean cotyledons, the cotyledons regained much of their chlorophyll, RNA, protein, and polyribosomes[9]. The leaves and stems of *S. sempervirens* became softer and exhibited high rooting ability after rejuvenation[10]. In the case of rejuvenated cotyledons in *Cucurbita pepo*, the polypeptide profile can fully recover, the photosynthesis rate can exceed that of juveniles, and the photochemical efficiency of PS also recovers gradually [11].

Phytohormones play an important role in plant phase change. Researchers have reported that zeatin-like cytokinin levels can be considered a marker for rejuvenation in rubber-trees[12], IAA and ABA levels were found to be higher in rejuvenated shoots than in mature shoots, whereas GA_3 and ZR levels exhibited the opposite tendency [13]. In *Malus xiaojinensis*, after successive in vitro subculture, the developmental stage of the explant material was reversed, the leaf IBA increased, and the ABA contents decreased. During the rejuvenation process, genes related to rooting, *CKI1*, *ARRO-1*, *ARF7* and *ARF19*, increased significantly[7]. In perennial woody plants, differentially expressed genes were also identified at different development stages[14]. These findings revealed that plant phase reversal is induced through regulation of gene expression or epigenetic modification.

sRNA has been certified as playing a key role in controlling plant development. miRNAs are 20–24 nucleotide non-coding RNAs that post-transcriptionally regulate gene expression by cleaving or inhibiting the translation of target gene transcripts [15]. miRNAs are evolutionarily conserved across plant lineages[16]. To date, miRNA156 and miRNA172 have been extensively studied in plant development. In maize phase changes, leaf morphogenesis changes and flowering ability are under the control of microRNA156, and its levels decline at the end of the juvenile phase[17]. In the case of arabidopsis, the duration of miRNA156 expression defines the juvenile phase and also regulates the timing of the juvenile to adult transition[18]. miRNA research involving reproductive development transitions has revealed that the amount of miR156 decreases and that of miRNA172 increases from the juvenile to the flowering phase. In the process, miR156 down-regulates its target genes, the *SPL* family of TFs, while miR172 down-regulates the target genes of the *AP2*-like family[19, 20]. The molecular mechanisms involved in the juvenile to adult transitions of trees and perennial woody plants have been identified [21]. However, the function of rejuvenation, which can be considered as the reverse, remains unclear.

Black locust(*R. pseudoacacia*)is a perennial deciduous tree species with fast growth and good resistance that originated in south-eastern North America. Black locust was first introduced to China in 1877, and developed successfully as an exotic species [22, 23]. In black locust plantations, there is a phenomenon in which individuals sprout from the roots of mother individuals that have reached a certain age. Without artificial intervention, root-sprout individuals can continue to grow and reach reproductive age. The root-sprout individuals are redeveloped from the root system of the mother tree. The root system of the plant is thought to have embryonic-stem-cell characteristics, so root-sprout individuals can be regarded as a form of phase reversal or rejuvenation[24]. The sprouted individuals share a root system with the original individuals. They have the same genotype and are affected by the same environment. This provides ideal material for studying the plant phase reversal of woody plants under asexual conditions. However,

compared to mother individuals, the growth characteristics, physiological characteristics, and molecular regulation mechanisms of rejuvenated individuals remain unclear.

In this study, we compared differences in leaf anatomical characteristics and inclusion content between the mother and rejuvenated individuals. mRNA and miRNA libraries constructed from the leaves of both rejuvenated and mother individuals were sequenced by high-throughput sequencing. After the comparison and in silico analysis, we addressed the following questions:) The growth and physiological characteristics of naturally rejuvenated black locust individuals.) The characteristics of transcription profile expression in the rejuvenation precession.) How miRNA is involved in regulating the black locust regeneration process. Elucidation of the physiological differences and molecular mechanism of black locust rejuvenation will provide theoretical support for natural phase reversal in plants.

Results

Anatomical characteristics of leaves

Comparing two individuals in the same group, all indicators in group A, except for SR, exhibited significant differences (Figure 1). In group B, the only significant differences were in palisade tissue thickness, CTR and leaf thickness. There were no differences in the thicknesses of the upper and lower epidermis between the two individuals in group C. Only the thickness of the palisade tissue, leaf thickness and CTR exhibited significant differences between groups A, B and C. These results show that there are stable and consistent differences between mother and rejuvenated individuals based on these three indicators. The mean values of the three indices indicate that, in the three indexes in the same group, the individual value of the older tree was larger than that of the younger tree.

Physiological characteristics of rejuvenated individuals

The results of the mean value analysis of physiological indices of different individuals showed that the trends in the MDA content, POD activity and Cu/Zn-SOD activity were inconsistent between different individuals in different groups (Figure 2). The total SOD (T-SOD) activity and soluble-sugar content followed the same trends in different individuals in different groups. That is, within the same group, the younger the rejuvenated individual, the lower the value. In the case of the total SOD activity, there were significant differences only between the C1 and C2 individuals. In the case of the soluble-sugar content, there were significant differences only between the B1 and B2 individuals.

Differences between hormone contents in leaves of rejuvenated individuals

Differences in the hormone contents of leaves in rejuvenated individuals in group B are taken as an example. Among the ABA, GA_3 and ZT indices, the results of the individual mean values indicate that

there were no consistent trends in the GA_3 and ABA/GA_3 contents between individuals of different ages (Figure 3). The ABA, ABA/ZT and GA_3/ZT contents of leaves decreased with the ages of rejuvenated individuals. The ZT contents increased with decreasing age of rejuvenated individuals.

Illumina paired-end sequencing and *de novo* assembly

In this study, after removing adaptors and low-quality data, a total of 982.7228M clean reads with a length of 150 bp were obtained from 24 libraries. Using overlapping information in high-quality reads, in total 1,571,388 transcripts were generated, with an average length of 946 bp and an N50 of 1,674. After comparing the different transcripts representing one unigene, the longest length transcript for each unigene was extracted. We obtained 175,862 unigenes in total. The average length was 1,423 bp and the N50 was 2,315.

Annotation of all non-redundant unigenes

Among the 175,862 unigenes, 124,217 (70.63%) were found to have significant similarities in terms of unique proteins. Of all of the unigenes, 92,832 (52.79%) with significant identities to SWISS-PROT proteins were matched to unique protein accessions. A smaller percentage was obtained when searching against the SWISS-PROT protein database than obtained against the NR database. In total, BLAST searches identified 91,758 unique protein accessions from the NR and SWISS-PROT protein databases, suggesting that our Illumina paired-end sequencing had likely captured a substantial proportion of the phase-reverse genes in *R. pseudoacasia*.

Functional classification by GO and cluster of orthologous groups (COG)

GO analysis was used to classify the functions of the predicted *R. pseudoacasia* unigenes. In total, 88,579 unigenes with BLAST matches to known proteins were assigned to GO classes. As shown in Figure 4, the majority of unigenes were assigned to the biological process categories, followed by cellular components and molecular functions. Under the category of biological processes, cellular processes (50,316, 25.06%) and metabolic processes (50,508, 25.16%) were prominently represented, indicating that important cellular processes and metabolic activities occur in *R. pseudoacacia* in response to rejuvenation. Under the classification of molecular functions, catalytic activity (46,803, 44.19%) and binding (44,652, 42.16%) made up the first and second largest categories, respectively, whereas other categories, such as those for signal transducer activity, nutrient reservoir activity, molecular function regulators, and others, together contained only 14,459 unigenes, representing 13.65% of the total number of unigenes. As for the cellular component, two categories, pertaining to cells and cell parts, accounted for approximately 40.73% of the cellular components identified. The membrane and membrane part

categories accounted for approximately 30.86% of the cellular component unigenes, and the organelle category accounted for 13.44%.

To predict and classify possible functions, all unigenes were aligned to the cluster of orthologous groups (COG) database, in which orthologous gene products are classified. Out of 124,217 unignes with significant similarity to NR proteins in this study, 80,086 sequences were assigned to COG classifications (Figure 5). Among the 24 COG categories, the cluster relating to general function prediction only (14,828, 18.52%) was the largest group, followed by those for replication, recombination and repair (8,583, 10.72%); transcription (8,359, 10.44%); and signal transduction mechanisms (7,637, 9.54%).

Functional classifications using KEGG pathways

To analyze the transcriptome of *R. pseudoacasia* further, all of the unigenes were analyzed with respect to the KEGG pathway database. Out of the 175,862 unigenes identified, 93,459 (53.14%) with significant matches to the database were assigned to six main categories (Figure 6). Among the six main categories identified, metabolism was the category with the largest number of unigenes, followed by genetic information processes, cellular processes, environment information processes, and organismal systems. These results indicate that active metabolic processes occur during the rejuvenation process. As shown in Figure 6, the KEGG metabolism category contained 11 sub-categories, including global and overview maps, carbohydrate metabolism, amino and metabolic diseases, and lipid metabolism, among others.

DEGs during the rejuvenation process

To reveal the molecular events that take place during rejuvenation, the expression levels of each gene in the samples and correlation coefficients were calculated so that we could evaluate the repeatability of our analysis. According to our results, the Pearson correlation coefficient between three replicas was 0.87~0.99 (Supporting Figure 1). The differential expression analysis showed that the number of DEGs varied between individuals in the same group (Figure 7). Among the DEGs in groups A and C, up-regulated genes were dominant, while down-regulated genes were dominant in group B. Hierarchical clustering analysis of the DEGs between groups B and C showed that, in group B, the DEGs of the three individuals of different ages exhibited a gradual trend (Figure 8). However, in group C, the up-regulated and down-regulated genes of C1 and C2 were similar, but differed from those of C3. The DEGs of the three individuals exhibited mutation patterns between C2 and C3. Analysis of the DEGs between individuals in group B and group C showed that none of the genes in group B varied continuously between the three age stages (Figure 9). Only one gene in group C varied continuously between the three age stages. Our analysis of DEGs between the rejuvenated and mother individuals in different groups showed that none of the genes exhibited the same differences between mother and rejuvenated individuals.

To elucidate the DEGs between mother and rejuvenated individuals of the same genotype, we carried out co-expression analysis of the DEGs. According to the number of DEGs, different correlation coefficients

(Spearman correlation coefficients = Scc) were set up to construct a co-expression network (Figure 10). Our co-expression analysis showed that there were some genes with high nodal degrees in the different groups that might play central roles in the regulation process (Support table 1).

GO term analysis of RNA-seq

To elucidate the functions of these DEGs, we carried out GO term analysis. In co-expression analysis, DEGs with nodal degrees greater than 10 were selected. The numbers of DEGs selected and annotations in different groups are shown in Supporting Table 2. The GO functional analysis of different groups showed that the two most enriched items in the biological process categories were cellular and metabolic processes. Cell parts and cells were the two most enriched items in the cellular category, and catalytic activity and binding were the two most enriched items in the molecular function category (Figure 11).

The KEGG pathway enrichment analysis of mRNA-seq

To understand the regulatory processes that the DEGs are involved in, the KEGG pathway was applied (Figure 12). The first three enriched pathways of the mother and rejuvenated individuals in group A were the global and overview maps, translation, folding, sorting and degradation. The first three pathways for the B1-B2 DEG enrichment in group B were the global and overview maps, translation, folding, sorting and deintegration. The first three pathways for B1-B3 DEG enrichment were the global and overview maps, carbohydrate metabolism, folding, sorting and degradation. The first three pathways for the C1-C2 DEG enrichment in group C were the global and overview maps, translation, and lipid metabolism. The first three pathways for the C1-C3 DEG enrichment were the global and overview maps, carbohydrate metabolism, and translation. This implies that these pathways and processes may participate in the rejuvenation process.

Deep-sequencing of sRNAs during rejuvenation

To investigate the role of miRNAs in mother and rejuvenated individuals, we constructed a total of 24 libraries. Each library was sequenced and the number of average unique sRNAs was 8,438,055, the average total number of sRNAs was 34,253,428. Using bowtie software to map sRNA to the reference genome obtained by transcriptome sequencing, an average of 1,255,390 (15.23%) unique sRNAs and 19,282,107 (56.29%) total sRNAs mapped to the reference genome in each sample (Support table 3). The length of the sRNAs in the 24 libraries ranged from 18–30 nt; the majority of sRNAs in each library were 21–24 nt in length (Figure 13), with 24 nt being the most common length of a unique sequence, followed by 21 nt.

Isolation of Known and Novel MiRNAs in black locust leaves

Unannotated unique sRNA sequences that matched perfectly to the assembly were used to identify known miRNAs. In total, 320 known miRNAs were identified in the 24 sRNA libraries. Unannotated sequences with no similarity to known miRNAs were used to predict novel miRNAs. In total, 671 novel miRNAs were identified. To compare the abundance of miRNAs in the process, the read counts were normalized to transcripts per million (TPM). As shown in Figure 14, miR2118 was the most abundantly expressed, while miR166a, miR167c, and miR2199 were moderately abundant.

Differentially expressed miRNAs between mother and rejuvenated individuals

To identify miRNAs associated with rejuvenation, the differentially expressed miRNAs in the mother and rejuvenated individuals were compared using a statistical method developed by Audic and Clacerie[25]. In total, 88 known and 220 novel miRNAs were differentially expressed in group A, 136 known and 305 novel miRNAs in group B, and 185 known and 295 novel miRNAs in group C. Among the different groups, C1 and C3 had the largest numbers of known and novel miRNAs, followed by B1 and B3 (Table 1). For known miRNAs in groups B and C, 9 and 26 miRNAs exhibited continuous differences in two rejuvenated individuals; 9 microRNAs exhibited common differences between mother and rejuvenated individuals in groups A, B and C (Figure 15, Supporting Table 4). In the case of novel miRNAs, 18 and 44 miRNAs exhibited continuous differences between the mother and rejuvenated individuals, and 7 novel miRNAs exhibited common differences between the mother and rejuvenated individuals in groups A, B and C (Figure 15, Supporting Table 4). Overall, in the same group, the numbers of microRNAs participating in the three stages were higher than the numbers of differences between the two stages alone. This result is inconsistent with the trends for differentially expressed genes at different ages. To find common expression patterns of the differentially expressed miRNAs, we performed hierarchical clustering based on the fold-change between different groups (Figure 16).

Table 1. Numbers of differentiated miRNAs

GO and KEGG analysis for target genes involved in rejuvenation

We predicted the target genes of known and novel miRNAs that were differentially expressed between individuals in groups A, B and C. The numbers of target genes predicted are shown in Supporting Table 5. Our GO term analysis for the target genes showed that, based on the biological process, the target genes for known (novel) processes are mainly involved in cellular and metabolic processes (Figure 17, Supporting Figure 2). Based on molecular function, of the target genes for 11 categories, the highest percentage of two categories for known and novel miRNAs were binding and catalytic activity. With respect to the cellular components, the target genes for the known and novel miRNAs were associated with 16 categories, the most common GO terms were for cells, cell parts, and membranes.

In the KEGG pathway analysis of target genes of known differentially expressed miRNAs, the three most abundant pathways in group A were the splicesome, Ras-signaling pathway, and protein processing in endoplasmic reticulum. The three most abundant pathways between B1 and B2 in group B were the spliceosome, RNA transport, and measles; and the three most abundant pathways between B1 and B3 were the splicesome, RNA transport, and protein processing in endoplasmic reticulum. The three most abundant pathways between C1 and C2 in group C were toxoplasmosis, measles, and influenza A; and the three most abundant pathways between C1 and C3 were toxoplasmosis, spliceosome, and measles. According to our KEGG pathway analysis of the target genes of novel differentially expressed miRNAs, the most enriched pathways in group A were the Ras-signaling pathway, MAPK signaling pathway, and peroxisome. The most abundant pathways of B1-B2 in group B were spliceosome, influenza A, plant hormone signal transduction, and RNA transport; and the most abundant pathways of B1-B3 were toxoplasmosis, measles, and the NF-Kappa B signaling pathway. In group C, the most abundant pathways in C1-C2 were toxoplasmosis, tuberculosis, and measles; and in C1-C3 they were toxoplasmosis, the NF-Kappa B signaling pathway, and spliceosome (Figure 18, Supporting Figure 3).

Association analysis of mRNA and predicted miRNA targets

Based on the gene information derived from the RNA-seq and miRNA targeted mRNAs in miRNA-seq, in total, 11 pairs of miRNA-RNA were detected based on the Pearson correlation coefficients (Pcc>0.9, p<0.05) of their expression and the targeting prediction relationship of the miRNA sequence (Supporting Table 6). Furthermore, negative regulation between miRNA and the predicted miRNA targets revealed that a total of 875 pairs of miRNA-mRNA pairs that changed in the opposite direction were identified between the rejuvenated and mother individuals in different groups (Figure 19, Supporting Table 7). In groups B and C, there were 7 miRNA-mRNA pairs exhibiting common differences between two rejuvenated and mother individual pairs, respectively (Supporting Table 8).

Discussion

The leaves of deciduous perennial trees are renewed every year, and their structures are comparable. The morphological and internal structures of leaves are closely related to plant photosynthesis, age, etc[26, 27]. Leaf thickness can be used as an indicator of material accumulation[28]. The thicker the leaf, the more organic matter the individual accumulates and the better the growth. Leaf thickening can prevent excessive transpiration of water, which is conducive to water conservation, and thus increase the water-use efficiency of the plant [29]. In this study, the leaf thicknesses of rejuvenated individuals were less than those of mother individuals, indicating that the rejuvenated individuals were weaker than the mother individuals in terms of organic matter accumulation and water-use efficiency. This difference may be because rejuvenated individuals do not have an independent root system and share roots with the mother individuals. The early formation of roots in mother individuals has advantages in terms of water absorption and material accumulation.

Highly developed palisade tissue can make leaf structures more compact and water-holding capacity stronger, and plant leaves with stronger resistance generally have more developed palisade tissue[30]. Previous studies have shown that electron transport, CO_2 fixation, and plastoquinone content are higher in palisade tissue than in other types of tissue[31]. The anatomical structures of the leaves used in this study showed that, under the same genetic background and environmental conditions, the younger the age of the tree, the smaller the thickness of the palisade tissue and the tightness of the leaves. The tightness of the leaf is the ratio of the thickness of the palisade tissue to the thickness of the leaf, which can further explain the development of palisade tissue in leaves. Our results show that the photosynthetic capacity of rejuvenated individuals may be inferior to that of mother individuals. However, this may be due to age differences. The minimum difference in tree age between rejuvenated individuals and mother individuals was 7 years. The youngest individuals in groups B and C were still in the seedling stage. Differences in leaf photosynthetic capacity can be caused by differences in tree age. Previous studies have found that there are differences in leaf photosynthetic capacity among individuals of different tree ages[32]. On the other hand, as rejuvenated individuals share the same root system as mother individuals, and rejuvenated individuals are younger than mother individuals, rejuvenated individuals may be at a disadvantage compared to mother individuals in terms of nutrient transport and absorption.

Under the influence of adverse environmental conditions, plants will produce excessive reactive oxygen species (ROS). If these are not removed, they will cause oxidative stress and damage the membrane system. To reduce oxidative damage, a set of ROS scavenging systems has formed in plants[33]. SOD, POD and CAT are important protective enzymes, especially SOD, which is considered one of the best antioxidants in the plant kingdom[34]. Accumulation of soluble sugar in plants can enhance osmotic regulation to maintain the water and swelling potential of cells, thus maintaining their normal function [35]. Studies have shown that soluble sugar is beneficial to the improvement of plant cold resistance[36]. Therefore, under the same conditions, differences in the SOD and soluble-sugar contents of individuals can reflect their growth status and ability to cope with stress. In this study, total SOD activity and soluble-sugar content were lower in the leaves of rejuvenated individuals than in those of mother individuals in each group. These results imply that, under the same conditions, the rejuvenated individuals were inferior to the mother individuals in terms of physiological metabolism and resistance. These conclusions are consistent with those drawn from our analysis of leaf anatomy.

Phytohormones are bioactive substances that can regulate the growth and development of plants in trace amounts [37]. They play an important role in cell division and elongation, maturation and senescence, dormancy and germination[38]. It is generally thought that ABA belongs to growth-inhibiting hormone, while GA_3 and Zeatin (ZT) belong to growth-stimulating hormone. ABA plays an important role in regulating plant resistance, maintaining the structure and function of cell membranes, and transporting substances in plants[39]. It has been reported that an increase in ABA content leads to a clear improvement in plant resistance[40]. The effect of CTK is contrary to that of ABA. ABA can promote plant senescence, while CTK can delay senescence[41]. The effects of hormones on the physiological activities of plants are related not only to the content of various hormones but also to the ratios of hormones, and

even the ratios of related hormones can play significant and important roles [42]. It has been observed that regulation of endogenous hormones in plants is determined not only by a single hormone but also is often the result of co-regulation of two or more hormones through antagonism or combined action[43]. For example, dry matter content and sugar accumulation are positively correlated with GA_3/ABA and IAA/ABA content ratios in *Helianthus tuberosus*, and the dynamic balance of endogenous hormones plays an important role in tuber development[44]. In this study, endogenous ABA content was higher in mother individuals than in rejuvenated individuals, whereas ZT content was lower in mother individuals than in rejuvenated individuals. The ABA and ZT contents of rejuvenated individuals of different ages indicated that the cell division and growth vigor of the younger individuals might be better than those of the mother individuals. The ratios of ABA/ZT and GA_3/ZT between different hormones showed that, the younger the rejuvenated individual, the smaller the ratio. We also observed that cell division and growth rates were higher with decreasing tree age, while resistance decreased with respect to that of the mother individual. Rejuvenated individuals have the same characteristics as young individuals, that is, they grow and develop fast, but their resistance to adverse environments is weak. The characteristics of rejuvenated individuals may be attributed to age differences, or they may be attributed to the existence of individual root systems and the non-uniformity of independent root systems.

In this study, we identified and investigated the expression profiles of mRNAs and miRNAs from mother and rejuvenated *R. pseudoacasia*. A large number of transcriptome unigenes (175,862) were sequenced using the Illumina HiSeq X Ten platform. The N50 length of the unigenes was 2,315 bp, and the average length was 1,423 bp. In total, 991 miRNAs containing 671 novel miRNAs were obtained. Compared to the previous study of *R. pseudoacacia*, the sequencing results obtained in this study provide longer unigenes, and the overall results are better than before[45-47]. Overall 131,359 (74.69%) of the identified unigenes were successfully annotated using BLAST searches of the public Nr, Nt, Swiss-prot, GO, COG and KEGG databases, given the absence of genomic information on *R. seudoacasia;* 86 (26.88%) out of 320 known miRNAs were detected based on 82 other species' miRNAs from miRBase 21.0 (Supporting Table 9). Notably, the percentage of predicted known miRNAs was lower than other studies in tree species [48]. It is possible that a larger percentage could not be predicted in this study due to the lack of a known *R. pseudoacasia* pool in miRBase*.*

The expression profiles of the mRNAs and miRNAs were further investigated to elucidate their possible roles in the rejuvenationof *R. pseudoacasia*. Extensive changes in gene expression and miRNA occur under phase change[49, 50]. In groups B and C, the younger the individual, the more differentially expressed genes were found between the rejuvenated and mother individuals. In groups A and C, more genes were up-regulated than were down-regulated. However, in group B, there were more down-regulated genes than up-regulated genes. Genotypes A and C exhibited a tendency to up-regulate genes, while genotype B exhibited a tendency to down-regulate genes. This indicates that, during the rejuvenation process, the overall upward or downward trends of genes are inconsistent, and there are differences between genotypes.

In groups B and C, there were two rejuvenated individuals from a mother tree. In the DEGs of the rejuvenated individuals, the mother trees of each group were used as the control; there were 209 overlapping genes in group B and 43 overlapping genes in group C. However, in any two-individual comparison within a group, there were no common DEGs in group B, and only one common DEG in group C. Our analysis of DEGs shared by rejuvenated individuals and their mother trees showed no common differences between different genotypes. The reason for this result is, on the one hand, that the genotypes of the three groups are inconsistent and there may be differences between genotypes during the rejuvenation process. On the other hand, because the ages of the three groups of rejuvenated individuals differed, there was specificity in gene expression at different ages, which is in agreement with the characteristics of the spatiotemporal expression of genes reported in previous studies[51]. Hierarchical clustering of DEGs between different individuals in group B showed that some genes exhibited continuous changes during the three age stages. However, in group C, the gene-expression patterns of C1 individuals were similar to those of C2 individuals, but quite different to those of C3 individuals. It is likely that the three tree ages (17 a, 10 a and 4 a) of group B were at different stages of growth and development, while in groups C, C1 (22 a) and C2 (17 a), the individuals may have been at the same stage of development, so the gene-expression patterns of the two groups were similar and significantly different to C3. Our co-expression analysis of DEGs showed that there were genes at the core of the regulatory network that were shared between different groups and individuals under the screening of different Spearman correlation coefficients. However, there were no overlapping regulatory events between different groups. This was related to the differences in the ages of the individuals in the different groups.

GO function analysis was carried out after screening the DEGs according to Scc. In the biological process class, the functions of the DEGs that were mainly enriched included cell metabolism, main metabolic processes, macromolecule biosynthesis processes and redox processes. In the cellular components class, the DEGs related to the membrane system were mainly enriched. In the molecular function class, the DEGs that were mainly enriched involved adenine nucleotide binding, ATP binding and protein kinase activity. The GO enrichment results show that, although there were differences between the different groups in terms of the DEGs during rejuvenation, and there were no common DEGs, the functions of the DEGs involved in rejuvenation were generally similar. These results further prove that gene expression is spatiotemporal, but with functional continuity. Rejuvenated individuals mainly exhibited differences in gene function related to metabolism and growth vigor. In the different groups, many genes involved in ketone synthesis and degradation pathways were identified in the KEGG pathway, including terpenoids, olefin fatty acids and other substances.

miRNAs such as miRNA156 and miRNA172 have been identified as playing important roles in plant phase change [52, 53]. However, the role of miRNAs in the rejuvenation of woody plants has rarely been studied. In this study, the highest expression levels were identified in micro2118, micro2118a-3p, micro166a and micro167c. Previous studies have shown that these miRNAs are involved in polarity formation during leaf development, and regulation of resistance genes[54, 55]. The length distribution of the miRNAs was mainly between 21 and 24 nt, which is consistent with previous studies[56]. There were two rejuvenated individuals in group B and group C; the differentially expressed miRNAs in group B did

not show the same trend as the DEGs, which increased with the age difference between the mother and the rejuvenated individual. According to our statistical analysis of miRNAs that were differentially expressed in the mother and rejuvenated individual, 60 known and 122 novel miRNAs overlapped during the two rejuvenation processes in group B. In group C, 69 known and 124 novel miRNAs overlapped during the two rejuvenation processes, which had the largest proportion of differentially expressed miRNAs (Figure 15). Unlike the DEGs in groups B and C, some of the differentially expressed miRNAs exhibited common differences in comparisons between any two individuals within a group. According to the comparisons between the rejuvenated individuals with different genotypes and their mother trees, nine known miRNAs and seven novel miRNAs exhibited common differences between genotypes.

These results indicate that there were some common differences in the expression of miRNAs between individuals of different ages, both within groups and between groups. This implies that miRNAs play key roles in the rejuvenation of *R. pseudoacasia.* We did not identify miR156 and miR172 in the common differentially expressed miRNAs of the rejuvenated individuals (Supporting Table 4). Rejuvenation is an inverse plant phase change process, and the molecular regulation mechanisms involved in this process may differ from the reported molecular regulation mechanisms of phase change. Some new molecular markers or small RNA markers that represent different stages of plant rejuvenation need to be investigated further. The experimental system used in this study was quite unusual, and *R. pseudoacacia* root germination samples were used as research material. Rejuvenated individuals always share part of their root system with their mother trees during their growth. In future research, we will investigate whether their development is affected by their mother trees or they exhibit different characteristics to those of ordinary phase change.

The GO analysis of differentially expressed known and novel microNA targets showed that, like the DEG GO analysis, cellular processes and metabolic processes are the most abundant target genes for miRNAs in both mother and rejuvenated individuals. The results show that the main biological processes of *R. pseudoacacia* during rejuvenation were the same, regardless of whether they were analyzed in terms of DEGs or miRNA target genes. Enrichment analysis of the KEGG pathway showed that the pathways of known microRNA target genes were mainly related to the synthesis and regulation of fatty acids, the biological contract between ketones and hormones, and related diseases. The pathways of the novel microRNA target genes were mainly related to ketone signal pathways, alkene biosynthesis, biological rhythm changes, and regulation of the pluripotency of stem cells.

Conclusions

We compared the leaf anatomical structures, physiological indexes, and hormone contents of mother trees and rejuvenated individuals of *R. pseudoacacia*. The thickness of the palisade tissue, leaflet thickness, and tightness of the leaflet structure exhibited stable differences between the mother trees and rejuvenated individuals. There was a consistent trend in the total SOD activity and soluble-sugar content of the mother and rejuvenated individuals of different genotypes. The ABA content, ZT content, ABA/ZT,

and GA_3/ZT exhibited the same trends in the two rejuvenated individuals in group B. From RNA-seq and microRNA-seq, in total, 175,862 unigenes, and 991 miRNAs, including 671 novel miRNAs, were identified. The DEGs between the mother tree and rejuvenated individuals in different genotypes differed, but the main functions of the DEGs in the different genotypes were the same. There were similarities between the mother trees and rejuvenated individuals with different genotypes in terms of differentially expressed miRNAs. These results imply that miRNAs may play key roles in black locust rejuvenation.

Finally, the experimental materials used in this study had the same genotype and were perennial. This experimental system can be used as ideal material for studying the rejuvenation of perennial woody plants, and has the advantage that herbaceous plants cannot develop continuously for many years. More research is required to understand the molecular mechanisms involved in plant rejuvenation. First, it will be helpful to elucidate the molecular mechanisms that regulate rejuvenation by using artificial methods to obtain rejuvenated individuals of the same age from mother trees of the same age. Second, there is a need to discover how microRNAs regulate the rejuvenation of *R. pseudoacacia* by combining downstream target genes and transcription factors that affect function in more detail.

Methods

Plant material and sampling strategy

We defined a mother individual and its root-sprouting individuals as a group. In the autumn of 2018, three groups were selected in *R. pseudoacacia* plantations at Lvcun State-owned Forest Farm, Luoning County, Henan Province, China (34°22' 40.8" N; 111°19' 48.6" E) and named groups A, B and C, respectively. The plant materials were formally identified by Shaoming Wang, director of Lvcun State-owned Forest Farm, and confirmed to be true and reliable. After the trees involved in the material were sampled, they are now in situ preserved in Lvcun State-owned Forest Farm and available at any time. In group A, two individuals with the same genotype were obtained; the older tree was denoted A1, and the younger tree was denoted A2. Similarly, group B contained three individuals with the same genotype, which were called B1, B2 and B3, and group C contained three individuals with the same genotype, denoted C1, C2 and C3. The ages of the individuals were estimated by drilling a wood core and counting the rings. Because B3 and C3 were too young, the tree age was estimated. Ten compound leaves were taken from the east, west, north and south sides of each individual crown. If there were no branches or leaves in one direction, at least three other directions were selected as three repetitions. Because the C3 individual was too young for us to distinguish the direction of the crown, three repetitions were taken from the top of the individual. We randomly selected a compound leaf from each direction. Five leaves in the upper part were used for mRNA-seq library construction and six leaves in the lower part were used for miRNA-seq library construction, then the samples were quickly stored in liquid nitrogen. Another compound leaf was randomly selected for use as anatomical material and stored in FAA fixative solution (95% ethanol/glacial acetic acid/formalin/distilled/distilled water=10:1:2:7). After mixing the remaining leaves, they were placed in an ice box and brought back to the laboratory for inclusion determination. Sampling methods and tree ages are shown in Figure 20 and Table 2.

Table 2 Experimental Samples and Sampling Direction

Leaf anatomy

Leaves of the A1, A2, B1, B2, C1, C2 individuals were used for leaf anatomy. The leaves were fixed for more than 24 h then taken out and dehydrated in ethanol series. Then, they were made transparent with xylene and embedded in paraffin. 8-μm cross sections were cut by microtome (LEICA RM2235). Slices were stained with safranin O-fast green and mounted in DPX. Images were obtained using a LEICA DMI40008 microscope. The thicknesses of the leaflet, upper epidermis, lower epidermis, palisade tissue and sponge tissue were calculated using Motic Image Plus2.0 software. Each index was based on the average of 30 observation values.

Tightness of leaflet structure (CTR) = palisade tissue thickness/leaflet thickness × 100%

Leaf tissue sparsity (SR) = sponge tissue thickness/leaflet thickness × 100%

Determination of physiological indicators

Leaves of the A1, A2, B1, B2, B3, C1 and C2 individuals were used to determine the physiological indices. The peroxidase (POD) activity, malondialdehyde (MDA) content, soluble-sugar content, copper-zinc-superoxide dismutase (Cu/Zn-SOD) and total superoxide dismutase (T-SOD) activity were evaluated using the A084-3, A003-3, A145, and A001-4 kits developed by the Nanjing Jiancheng Institute of Bioengineering, according to the manufacturer's protocol for each kit. Three repeat measurements were taken for each individual in one sampling direction.

Hormone content determination

The leaves of the B1, B2 and B3 individuals were used for hormone content determination. The abscisic acid (ABA), gibberellin (GA_3) and zeatin (ZT) contents were analyzed by ultra-high-performance liquid chromatography tandem mass spectrometry (UPLC-MS/MS). The sample pretreatment steps were as follows: after the leaves had been ground in liquid nitrogen, 50 mg (with a precision of four decimal places) was weighed and placed in a 2-ml centrifugal tube to record the net weight of the sample. Then we added 0.5 ml pyrolysis solution (isopropanol: H_2O: HCl = 2:1:0.002) and ABA, GA_3, ZT isotope internal standard. The samples were vibrated at 4°C for 30 minutes, 1 ml dichloromethane was added, and vibration continued for a further 30 minutes. Next, they were centrifuged for 10 minutes at 13 000 rpm; the clear liquid was then steamed on a nitrogen blower. After adding 0.1 ml methanol water and centrifuging for 10 minutes at 13000 rpm, we placed the supernatant in the machine (UPLC-MS/MS) for detection. Each index measurement was repeated three times for each individual.

Library construction and sequencing of mRNA and small RNA

Leaves from A1, A2, B1, B2, B3, C1, C2 and C3 individuals were used for RNA extraction and sequencing. Samples from three directions were selected for each individual. The total RNA was extracted from the leaves using TRIziol reagent (Invitrogen, Carlsbad, CA, USA) according to the manufacturer's protocol. The quality and quantity of the RNA were evaluated by Agilent2100 Bioanalyzer (Agilent Technologies, Waldbroom, Germany) and spectrophotometry (SmartSpec Plus, Bio-Rad, USA), respectively. The transcriptome sequencing library was generated using NEBNext Ultra RNA Library Prep Kits for Illumina (NEB, USA) following the manufacturer's instructions. Following the instructions provided by Illumina, the mRNA was enriched by Oligo (dT). Fragmentation buffer was added to disrupt the mRNA into short fragments. Reverse transcriptase and random primers were used to synthesize the first strand cDNA from the cleaved mRNA fragments. The second strand cDNA was synthesized using buffer, dNTPs, RNase H, and DNA polymerase □. The double strand cDNA was purified using QIAquick PCR extraction kits (QIAGEN, Hilden, Germany) and washed with EB buffer for end repair and single nucleotide A (adenine) addition. Finally, sequencing adaptors were ligated onto the fragments. The required fragments were purified by AMPure XP beads and enriched by the polymerase chain reaction (PCR) to construct a library for transcriptome sequencing.

For small RNA library construction, RNA was fractionated on a 15% denaturing polyacrylamide gel. sRNA regions corresponding to 18–30nt were excised and recovered. These sRNAs were then 5' and 3' RNA adapter-ligated using T4 RNA ligase (Takara, Dalian, China). Ligated products were purified using an Oligotex mRNA mini kit (Qiagen, Hilden, Germany) and subsequently transcribed into cDNAs via a SuperScript □ RT (Invitrogen, USA). PCR amplifications were performed with primers annealed to the ends of the adapters. The final quality of the cDNA library was ensured using an Agilent2100 Bioanalyzer (Agilent Technologies, Santa Clara, CA, USA) and we verified its size, purity, and concentration. The transcriptome library and small RNA library PCR products were sequenced using the Illumina HiSeq X Ten platform (Illumina, San Diego, CA, USA).

Data filtering and *de novo* sequence assembly

The sequencing-received raw image data were transformed by base calling into raw sequence data, which were termed raw reads. The raw data were then filtered by data-processing steps to generate clean data via a process that included the removal of adapter sequences, reads in which more than unknown base N were greater than 5%, and low-quality sequences (in which the percentage of low-quality bases, with quality value≤10, was greater than 20%). After the clean reads had been generated, a transcript assembly was obtained using the Trinity software with min_kmer_cov set to 3 by default and all other parameters set to the default values. Then Tgicl was used to cluster transcripts to obtain the unigene. The raw data are available in the NCBI Sequence Read Archive repository (https://www.ncbi.nlm.nih.gov/sra/) under accession number PRJNA542041.

Functional annotation of unigenes

For functional annotation, the unigenes that might putatively encode proteins were searched against the NR (http://www.ncbi.nlm.nih.gov/), NT (http://www.ncbi.nlm.nih.gov/), Swiss-Prot (http://www.ebi.ac.uk/uniprot/), KEGG (http://www.genome.jp/kegg/) and COG (http://www.ncbi.nlm.nih.gov/COG/) databases using the BLASTX algorithm[57]. A typical cut-off value of E-value<1e-5 was used. In the case of the NR annotations, the Blast2GO v2.5 software was used to assign GO annotations to the unigenes according to the component function, biological process and cellular component ontologies[58]. A typical cut-off value of E-value<1e-6 was used.

Identification of differentially expressed unigenes

Bowtie2 was used to map clean reads to assembled reference sequences, and then RSEM was used to calculate the expression levels of transcripts[59]. The expression levels of different genes were expressed in terms of the fragments per kilobase of transcript per million mapped reads (FPKM) value[60]. After calculating the gene expression levels, the differentially expressed genes (DEGs) were screened by comparing the gene expression levels. Implementing the method described by Tarazona[61], differential expression analysis of individuals in each group was performed using the DESeq2 R package (1.10.1). DESeq2 provides statistical routines for determining differential expression in digital gene-expression data using a model based on the negative binomial distribution. In this study, unigenes with an adjusted P≤0.05 identified by DESeq2 were considered differentially expressed. According to the GO and KEGG annotation results and official classification, enrichment analysis was carried out using the Phyper function in R. The functional divergence ratio (FDR) and correction of *p*-values were evaluated and FDR ≤0.01 was regarded as significant enrichment.

Bioinformatics analysis and miRNA identification

Sequence tags from deep sequencing were processed by Phred and Crossmatch (http://www.phrap.org/phredphrapconsed.html), filtering out low-quality tags and eliminating contamination of adaptor sequences not ligated to any other sequences. The remaining high-quality sRNA reads were trimmed from their adapter sequences. rRNAs, scRNA, snoRNA, snRNA and tRNA were removed from the sRNA sequences through a BLASTn search using the NCBI Genebank database (http://www.ncbi.nlm.nih.gov/blast/Blast.cgi/) and Rfam(11.0) database (http://www.sanger.ac.uk/resources/databases/rfam.html) using the following program and parameters: blastall –p blastn –F F –e0.01. All annotations were summarized using tag2annotation software (developed by BGI) in the following order of preference: rRNA(Genbank>Rfam3)>known miRNA>piRNA>repeat>exon>intron. The remaining sequences were aligned to known plant miRNAs from miRbase22 (http://www.birbase.org/) with up to two mismatches. Reads that were not annotated were used to predict novel miRNAs using Mireap (http://sourceforge.net/projects/mireap/), prediction software developed by the BGI, by screening the biological characteristics of miRNAs. The raw data are available in the NCBI Sequence Read Archive repository (https://www.ncbi.nlm.nih.gov/sra/) under accession number PRJNA543377.

Differential expression analysis of miRNAs

The frequency of each identified miRNA read count was normalized according to the expression of transcripts per million (TPM) to the total clean miRNA reads in each sample. The fold-change of miRNA expression between the rejuvenated individual and mother individual in each group was calculated as $\log_2$(rejuvenation/mother). The DESeq2 R package was used to determine whether there was a significant difference in expression between the two samples. The *P*-value was≤0.05 and, with a normalized sequence count $\log_2$(rejuvenation/mother)>1 or <-1, the specific miRNA was considered differentially expressed.

Target prediction of miRNAs

Target prediction of miRNAs was performed by TargetFinder (http://github.con/carringtonlab/TargetFinder) and psRNA Target software (http://plantgrn.nobe.org/psRNATarget/). The default parameters were selected for candidate target prediction. Genes that overlapped between the two software applications were regarded as target genes, for which we then carried out enrichment analysis using GO terms and KEGG pathways.

Abbreviations

SOD: Superoxide dismutase; ABA: Abscisic acid; ZT: Zeatin; GA_3: Gibberellin A3; ZR: Zeatin-riboside; CTK: Cytokinin; GO: Gene Ontology; KEGG: Kyoto Encyclopedia of Genes and Genomes; FDR: False discovery rate; PS□: Photosystem□; IAA: Auxin; TFs: Transcription factors; SR: Leaf tissue sparsity; CTR: Tightness of leaflet structure; MDA: Malondialdehyde; POD: Peroxidase; CAT: Catalase; COG: Cluster of orthologous groups; BLAST: Basic Local Alignment Search Tool; DEGs: Differentially expressed genes; Scc: Spearman correlation coefficients; TPM: Transcripts per million; Pcc: Pearson correlation coefficients; ROS: Reactive oxygen species; DPX: Mountant for histology; UPLC-MS/MS: Ultra-high-performance liquid chromatography tandem mass spectrometry; FPKM: Fragments per kilobase of transcript per million.

Declarations

Acknowledgements

We thank Shaoming Wang and other members of the forest farm in Lvcun, Luoning county, He'nan province for their help in samples identification and collection. We also thank other students in our lab for their help in the daily work.

Funding

This study was funded by the Major Scientific Research Achievements Cultivation Project of Beijing Forestry University(2017CGP007); National Nature Science Foundation of China (31570677); the

National Key R&D Program of China (2017YFD0600503) and the Long-Term Research Program for Young Teachers of Beijing Forestry University (2015ZCQ-SW-03).

Availability of data and material

The datasets generated and/or analyzed during the current study have been deposited in the NCBI Sequence Read Archive repository, with BioProject accession number PRJNA542041, and PRJNA543377 (https://www.ncbi.nlm.nih.gov/bioproject). Any reasonable requests are available from the corresponding author.

Authors' contributions

YL and JP conceived the research; ZZ designed and performed the experiments, analyzed data and drafted the manuscript; YS and CH participated in coordination of the study; LD and QG performed leaf anatomy; XL and SC analyzed a part of mRNA-seq data; SD and ZM analyzed a part of miRNA-seq data. All authors read and approved the final manuscript.

Competing interests

The authors declare that they have no competing interests

Ethics approval and consent to participate

Not applicable

Consent for publication

Not applicable

The English in this manuscript has been checked by at least two professional editors, both native speakers of English. For a certificate, please see:

http://www.textcheck.com/certificate/PKKhPq

Additional File Legend

Table S1: Node degree of DEGs in co-expression network.

Table S2: Number of selected DEGs and GO term annotation.

Table S3: Comparison statistics of small RNA to reference genome.

Table S4: Common differential miRNAs between mother trees and rejuvenated individuals in three groups

Table S5: The number of target genes predicted by differential expressed miRNA.

Table S6: Association analysis of miRNA-mRNA based on mRNA-seq and miRNA-seq.

Table S7: Negative regulation pairs of miRNA-mRNA between mother trees and rejuvenated individuals.

Table S8: Overlapping miRNA-mRNA pairs in group B and C during two rejuvenation process.

Table S9: Family analysis of known miRNAs.

Figure S1: Correlation coefficient between samples (method = pearson).

Figure S2: GO annotation of novel miRNA target genes.

Figure S3: KEGG Enrichment of novel miRNA target genes.

References

1.Basheer-Salimia R: Juvenility, Maturity, and Rejuvenation in Woody Plants. *Herbron University Research Journal* 2007, 3(1):17-43.

2.Heide OM: Juvenility, maturation and rejuvenation in plants: adventitious bud formation as a novel rejuvenation process. *The Journal of Horticultural Science and Biotechnology* 2018:1-10.

3.HAMMATT N, GRANT NJ: Apparent Rejuvenation of Mature Wild Cherry (Prunus avium L.) during Micropropagation. *PLANT BIOLOGY* 1993.

4.Huang LC, Lin LY, Chen CM, Chen LJ, Huang BL, Murashige T: Phase reversal in Sequoia sempervirens in relation to mtDNA. *PHYSIOL PLANTARUM* 2010, 94(3):379-383.

5.Guleria V, Vashisht A: Rejuvenation and Adventitious Rooting in Shoot Cuttings of Tectona Grandis under Protected Conditions in New Locality of Western Himalayas. *Universal journal of Plant Science* 2014, 2(6):103-106.

6.Martínez T, Vidal N, Ballester A, Vieitez AM: Improved organogenic capacity of shoot cultures from mature pedunculate oak trees through somatic embryogenesis as rejuvenation technique. *Trees* 2012, 26(2):321-330.

7.Xiao Z, Ji N, Zhang X, Zhang Y, Wang Y, Wu T, Xu X, Han Z: The lose of juvenility elicits adventitious rooting recalcitrance in apple rootstocks. *Plant Cell Tissue & Organ Culture* 2014, 119(1):51-63.

8.Mirschel F, Zerbe S, Jansen F: Driving factors for natural tree rejuvenation in anthropogenic pine (Pinus sylvestris L.) forests of NE Germany. *FOREST ECOL MANAG* 2011, 261(3):683-694.

9.Skadsen RW, Cherry JH: Quantitative changes in in vitro and in vivo protein synthesis in aging and rejuvenated soybean cotyledons. *PLANT PHYSIOL* 1983, 71(4):861-868.

10.Huang LC, Lius S, Huang BL, Murashige T, Mahdi El FM, Van GR: Rejuvenation of Sequoia sempervirens by Repeated Grafting of Shoot Tips onto Juvenile Rootstocks in Vitro: Model for Phase Reversal of Trees. *PLANT PHYSIOL* 1992, 98(1):166-173.

11.Ananieva K, Ananiev ED, Mishev K, Georgieva K, Tzvetkova N, Van Staden J: Changes in photosynthetic capacity and polypeptide patterns during natural senescence and rejuvenation of Cucurbita pepo L. (zucchini) cotyledons. *PLANT GROWTH REGUL* 2008, 54(1):23-29.

12.Perrin Y, Doumas P, Lardets L, Carrons M: Endogenous cytokinins as biochemical markers of rubber-tree (Hevea brasiliensis) clone rejuvenation. *Plant Cell, Tissue and Organ Culture* 1997, 47(3):239-245.

13.Liu H, Gao Y, Song X, Ma Q, Zhang J, Pei D: A novel rejuvenation approach to induce endohormones and improve rhizogenesis in mature Juglans tree. *PLANT METHODS* 2018, 14(1):13.

14.Gao Y, Yang FQ, Cao X, Li CM, Wang Y, Zhao YB, Zeng GJ, Chen DM, Han ZH, Zhang XZ: Differences in Gene Expression and Regulation during Ontogenetic Phase Change in Apple Seedlings. *PLANT MOL BIOL REP* 2014, 32(2):357-371.

15.Axtell M, Snyder J, Bartell D: Common functions for diverse small RNAs of land plants. *The Plant Cell* 2007, 19(6):1750-1769.

16.Yakovlev IA, Carl Gunnar F, Ystein J: MicroRNAs, the epigenetic memory and climatic adaptation in Norway spruce. *NEW PHYTOL* 2010, 187(4):1154-1169.

17.Beydler BD, Osadchuk K, Cheng CL, Manak JR, Irish EE: The juvenile phase of maize sees upregulation of stress-response genes and is extended by exogenous JA. *PLANT PHYSIOL* 2016, 171(4):2648-2658.

18.Wu G, Park MY, Conway SR, Wang J, Weigel D, Poethig RS: The Sequential Action of miR156 and miR172 Regulates Developmental Timing in *Arabidopsis*. *CELL* 2009, 138(4):750-759.

19.Tang STG: To Bloom or Not to Bloom Role of MicroRNAs in Plant Flowering. *MOL PLANT* 2015, 8(3):359-377.

20.Jia-Wei W, Benjamin C, Detlef W: miR156-regulated SPL transcription factors define an endogenous flowering pathway in Arabidopsis thaliana. *CELL* 2009, 138(4):738-749.

21.Wang JW, Park MY, Wang LJ, Koo Y, Chen XY, Weigel D, Poethig RS: miRNA control of vegetative phase change in trees. *PLOS GENET* 2011, 7(2):e1002012.

22.Straker KC, Quinn LD, Voigt TB, Lee DK, Kling GJ: Black Locust as a Bioenergy Feedstock: a Review. *BIOENERG RES* 2015, 8(3):1117-1135.

23.Nan L, Li D, Bo W, Yue Z, Luo Z, Xun S, Sun Y, Yun L: A preliminary study on the crossability in Robinia pseudoacacia L. *EUPHYTICA* 2015, 206(3):555-566.

24.Crawford BC, Sewell J, Golembeski G, Roshan C, Long JA, Yanofsky MF: Plant development. Genetic control of distal stem cell fate within root and embryonic meristems. *SCIENCE* 2015, 347(6222):655-659.

25.Audic S, Claverie JM: The significance of digital gene expression profiles. *GENOME RES* 1997, 7(10):986-995.

26.Cao KF, Booth EW: Leaf anatomical structure and photosynthetic induction for seedlings of five dipterocarp species under contrasting light conditions in a Bornean heath forest. *J TROP ECOL* 2001, 17(2

):163-175.

27.Jia X, Wang G, Wang F, Li Y, Xu Z, Xiong A: Anatomic Structure and Expression Profiles of Related Genes: Novel Insights into Leaf Development in Celery. *J PLANT GROWTH REGUL* 2015, 34(3):519-531.

28.Hanba YT, Miyazawa SI, Terashima I: The Influence of Leaf Thickness on the CO2 Transfer Conductance and Leaf Stable Carbon Isotope Ratio for Some Evergreen Tree Species in Japanese Warm-Temperate Forests. *FUNCT ECOL* 1999, 13(5

):632-639.

29.Búrquez A: Leaf Thickness and Water Deficit in Plants: A Tool for Field Studies. *J EXP BOT* 1987, 38(186):109-114.

30.Terashima I, Inoue Y: Comparative Photosynthetic Properties of Palisade Tissue Chloroplasts and Spongy Tissue Chloroplasts of Camellia japonica L.: Functional Adjustment of the Photosynthetic Apparatus to Light Environment within a Leaf. *Plant & Cell Physiology* 1984, 25(4):555-563.

31.Terashima I, Inoue Y: Palisade Tissue Chloroplasts and Spongy Tissue Chloroplasts in Spinach: Biochemical and Ultrastructural Differences. *Plant & Cell Physiology* 1985, 26(1):63-75.

32.Katahata SI, Naramoto M, Kakubari Y, Mukai Y: Seasonal changes in photosynthesis and nitrogen allocation in leaves of different ages in evergreen understory shrubDaphniphyllum humile. *Trees* 2007, 21(6):619-629.

33.Kaur N, Dhawan M, Sharma I, Pati PK: Interdependency of Reactive Oxygen Species generating and scavenging system in salt sensitive and salt tolerant cultivars of rice. *BMC PLANT BIOL* 2016, 16(1):131.

34.Bowler C, Camp WV, Montagu MV, Inzé D, Asada K: Superoxide Dismutase in Plants. *CRIT REV PLANT SCI* 1994, 13(3):199-218.

35.Couée I, Sulmon C, Gouesbet G, El Amrani A: Involvement of soluble sugars in reactive oxygen species balance and responses to oxidative stress in plants. *J EXP BOT* 2006, 57(3):449-459.

36.Ma YY, Zhang Y, Jiang L, Shao HB: Roles of plant soluble sugars and their responses to plant cold stress. *African Journal of Biotechnology* 2009, 8(10):2004-2010.

37.Davies PJ: Plant Hormones and their Role in Plant Growth and Development; 1987.

38.Santner A, Calderon-Villalobos L, Estelle M: Plant hormones are versatile chemical regulators of plant growth. *NAT CHEM BIOL* 2009, 5(5):301-307.

39.Hirayama T, Shinozaki K: Perception and transduction of abscisic acid signals: keys to the function of the versatile plant hormone ABA. *TRENDS PLANT SCI* 2007, 12(8):343-351.

40.Yao Y, Dong CH, Yi Y, Xiang L, Zhang X, Liu J: Regulatory function of AMP1 in ABA biosynthesis and drought resistance in arabidopsis. *J PLANT BIOL* 2014, 57(2):117-126.

41.Wu L, Ma N, Jia Y, Zhang Y, Feng M, Jiang C, Ma C, Gao J: An Ethylene-Induced Regulatory Module Delays Flower Senescence by Regulating Cytokinin Content. *PLANT PHYSIOL* 2017, 173(1):853-862.

42.Albert L: Methods for improving growth and crop productivity of plants by adjusting plant hormone levels, ratios and/or co-factors. *Stoller Enterprises* 2006.

43.Han H, Tian Z, Fan Y, Cui Y, Cai J, Jiang D, Cao W, Dai T: Water-deficit treatment followed by re-watering stimulates seminal root growth associated with hormone balance and photosynthesis in wheat (Triticum aestivum L.) seedlings. *PLANT GROWTH REGUL* 2015, 77(2):201-210.

44.Li L, Shao T, Yang H, Chen M, Gao X, Long X, Shao H, Liu Z, Rengel Z: The endogenous plant hormones and ratios regulate sugar and dry matter accumulation in Jerusalem artichoke in salt-soil. *SCI TOTAL ENVIRON* 2017, 578:40-46.

45.Quan J, Meng S, Guo E, Zhang S, Zhao Z, Yang X: De novo sequencing and comparative transcriptome analysis of adventitious root development induced by exogenous indole-3-butyric acid in cuttings of tetraploid black locust. *BMC GENOMICS* 2017, 18(1):179.

46.Wang JX, Lu C, Yuan CQ, Cui BB, Qiu QD, Sun P, Hu RY, Wu DC, Sun YH, Li Y: Characterization of ESTs from black locust for gene discovery and marker development. *Genetics & Molecular Research Gmr* 2015, 14(4):12684.

47.Lu N, Dai L, Luo Z, Wang S, Wen Y, Duan H, Hou R, Sun Y, Li Y: Characterization of the Transcriptome and Gene Expression of Tetraploid Black Locust Cuttings in Response to Etiolation. *GENES-BASEL* 2017, 8(12):345.

48.Ma C, Qi Y, Liang W, Yang L, Lu Y, Guo P, Ye X, Chen L: MicroRNA Regulatory Mechanisms on Citrus sinensis leaves to Magnesium-Deficiency. *FRONT PLANT SCI* 2016, 7(232):201.

49.Silva AT, Ribone PA, Chan RL, Ligterink W, Hilhorst HW: A Predictive Coexpression Network Identifies Novel Genes Controlling the Seed-to-Seedling Phase Transition in Arabidopsis thaliana. *PLANT PHYSIOL* 2016, 170(4):2218-2231.

50.Xing L, Dong Z, Li Y, Zhao C, Zhang S, Shen Y, Na A, Han M: Genome-wide identification of vegetative phase transition-associated microRNAs and target predictions using degradome sequencing in Malus hupehensis. *BMC GENOMICS* 2014, 15(1):1125.

51.Kloosterman B, Vorst O, Hall RD, Visser RG, Bachem CW: Tuber on a chip: differential gene expression during potato tuber development. *PLANT BIOTECHNOL J* 2010, 3(5):505-519.

52.Dã Az-Manzano FE, Cabrera J, Ripoll JJ, Del OI, Andrã S MF, Silva AC, Barcala M, Sã NM, Ruã Z-Ferrer V, De AJ: A role for the gene regulatory module microRNA172/TARGET OF EARLY ACTIVATION TAGGED 1/FLOWERING LOCUS T (miRNA172/TOE1/FT) in the feeding sites induced by Meloidogyne javanica in Arabidopsis thaliana. *NEW PHYTOL* 2018, 217(2).

53.Gandikota M, Birkenbihl RP, Höhmann S, Cardon GH, Saedler H, Huijser P: The miRNA156/157 recognition element in the 3' UTR of the Arabidopsis SBP box gene SPL3 prevents early flowering by translational inhibition in seedlings. *PLANT J* 2010, 49(4):683-693.

54.de Vries S, Kloesges T, Rose LE: Evolutionarily Dynamic, but Robust, Targeting of Resistance Genes by the miR482/2118 Gene Family in the Solanaceae. *GENOME BIOL EVOL* 2015, 7(12):3307-3321.

55.Xiaozhen Y, Hua W, Hong L, Zhenhuan Y, Fupeng L, Li Y, Hai H: Two types of cis-acting elements control the abaxial epidermis-specific transcription of the MIR165a and MIR166a genes. *FEBS LETT* 2009, 583(22):3711-3717.

56.Jeong D: Functional diversity of microRNA variants in plants. *J PLANT BIOL* 2016, 59(4):303-310.

57.Lobo I: Basic Local Alignment Search Tool (BLAST). *J MOL BIOL* 2012, 215(3):403-410.

58.Ana C, Stefan GT, Juan Miguel GG, Javier T, Manuel T, Montserrat R: Blast2GO: a universal tool for annotation, visualization and analysis in functional genomics research. *BIOINFORMATICS* 2005, 21(18):3674-3676.

59.Langmead B, Salzberg SL: Fast gapped-read alignment with Bowtie 2. *NAT METHODS* 2012, 9(4):357-359.

60.Florea L, Song L, Salzberg SL: Thousands of exon skipping events differentiate among splicing patterns in sixteen human tissues. *F1000res* 2013, 2:188.

61.Tarazona S, Garcíaalcalde F, Dopazo J, Ferrer A, Conesa A: Differential expression in RNA-seq: A matter of depth. *GENOME RES* 2011, 21(12):2213-2223.

Tables

Table 1. Numbers of differentiated miRNAs

	Known			Novel		
	Total	Up	Down	Total	Up	Down
A1 vs. A2	88	23	65	220	100	120
B1 vs. B2	92	53	39	214	99	115
B1 vs. B3	101	51	60	209	98	111
B2 vs. B3	71	22	49	187	93	94
C1 vs. C2	93	64	29	192	90	102
C1 vs. C3	153	109	44	224	111	113
C2 vs. C3	121	78	43	205	106	99

Table 2 Experimental Samples and Sampling Direction

Group	Serial number	Age	Sampling direction
A	A1	21a	E、S、W、N
	A2	14a	E、S、W、N
B	B1	17a	E、S、W、N
	B2	10a	N、S、W
	B3	4a	N、S、W
C	C1	22a	E、S、W、N
	C2	17a	E、S、W、N
	C3	3a	T1、T2、T3

Note: E stands for east, S for south, W for west, N for north, T1, T2, T3 for three repetitions.

Figures

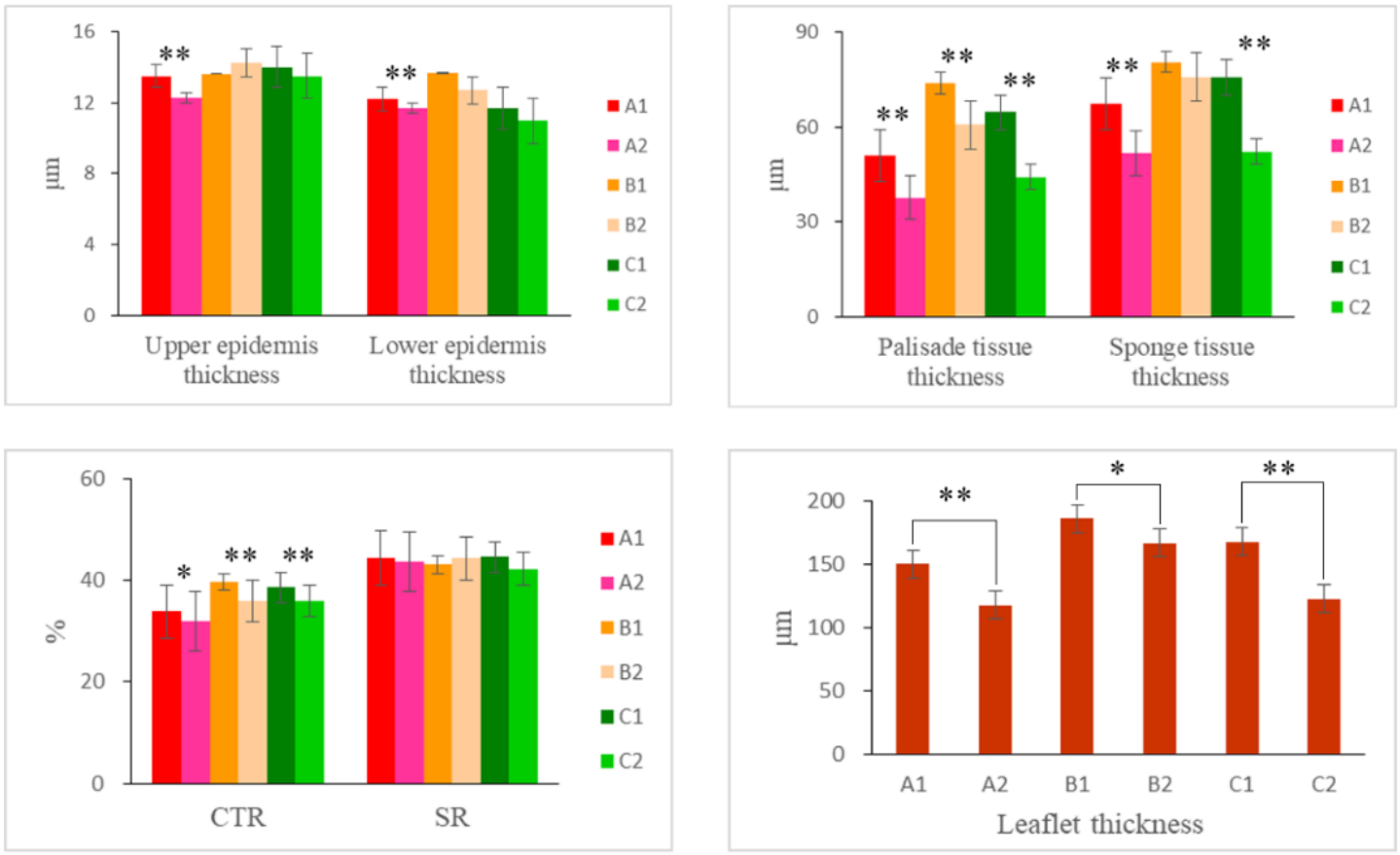

Figure 1

Mean and difference analysis of leaf anatomical indicators. * represents 0.01≤ P <0.05, ** represents P<0.01.

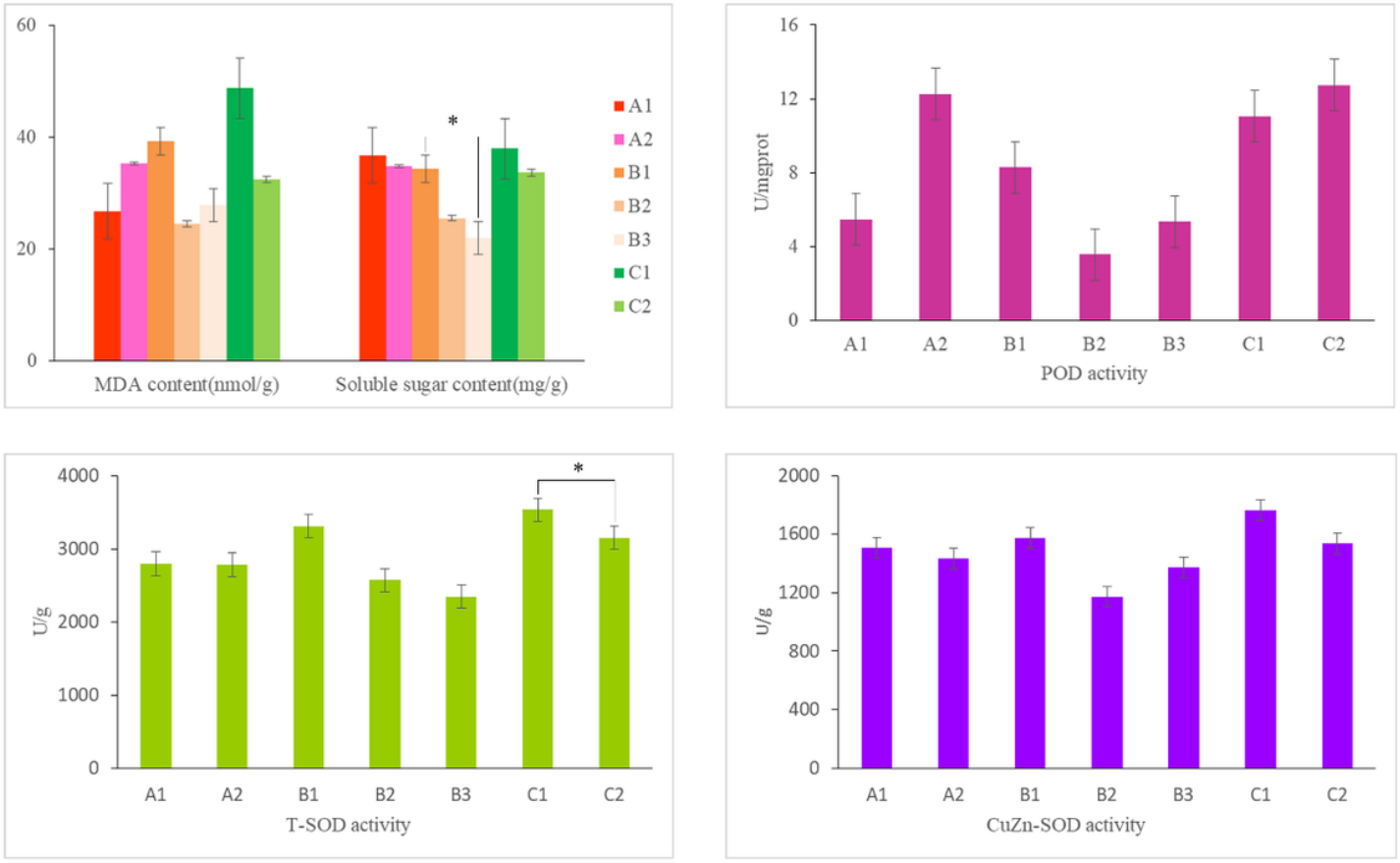

Figure 2

Mean and difference analysis of physiological index. * represents 0.01≤ P <0.05

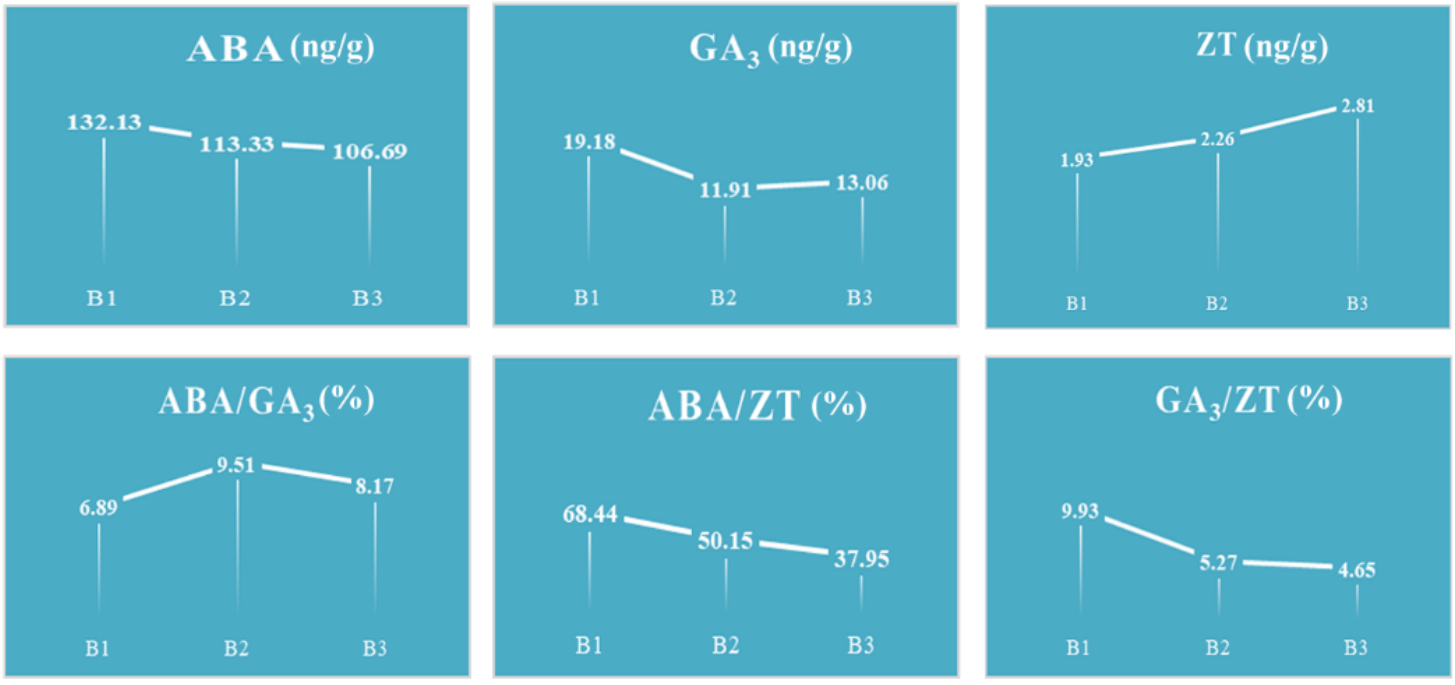

Figure 3

Average hormone content of leaves

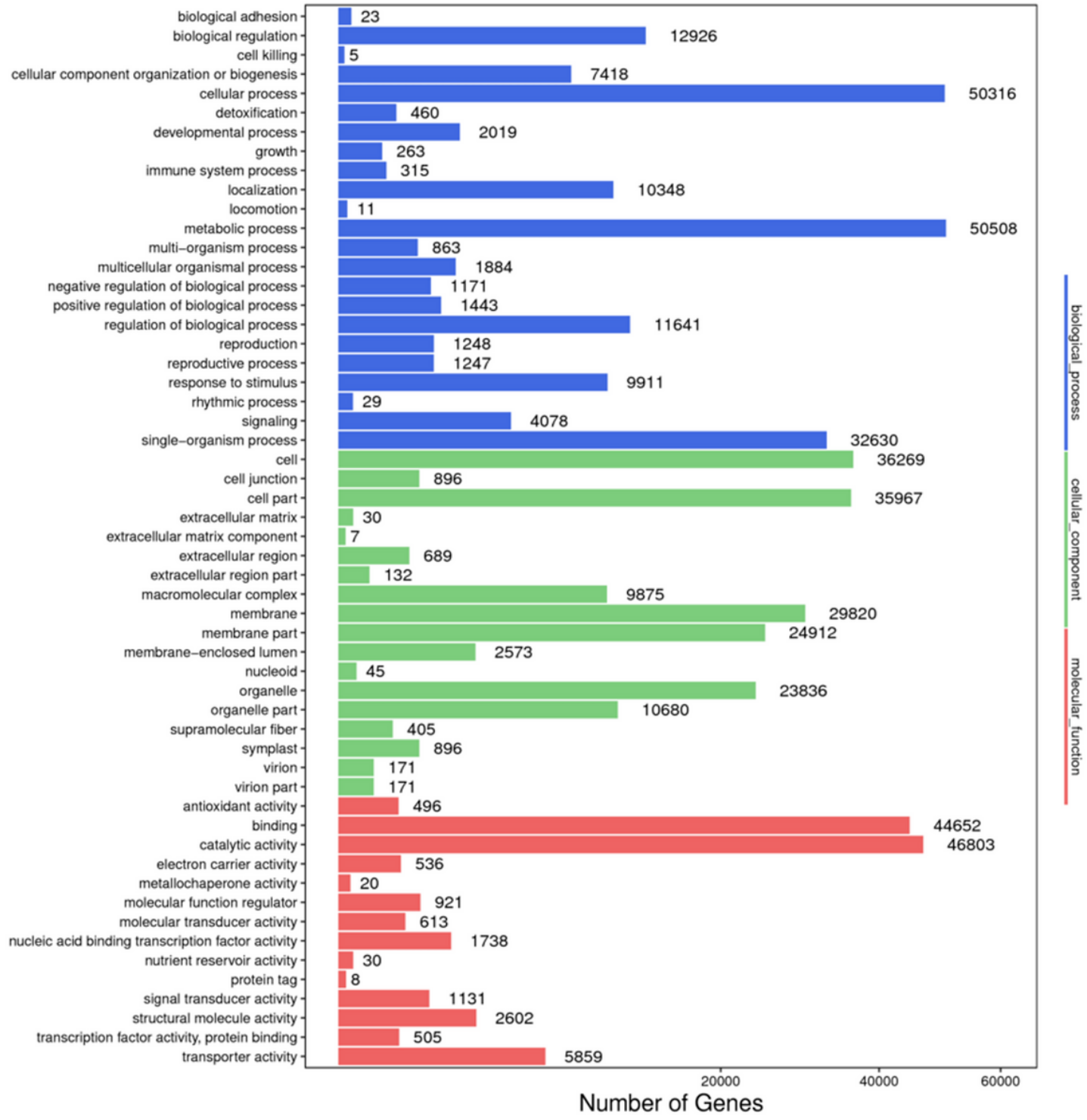

Figure 4

Unigene functions classified by gene ontology (GO)

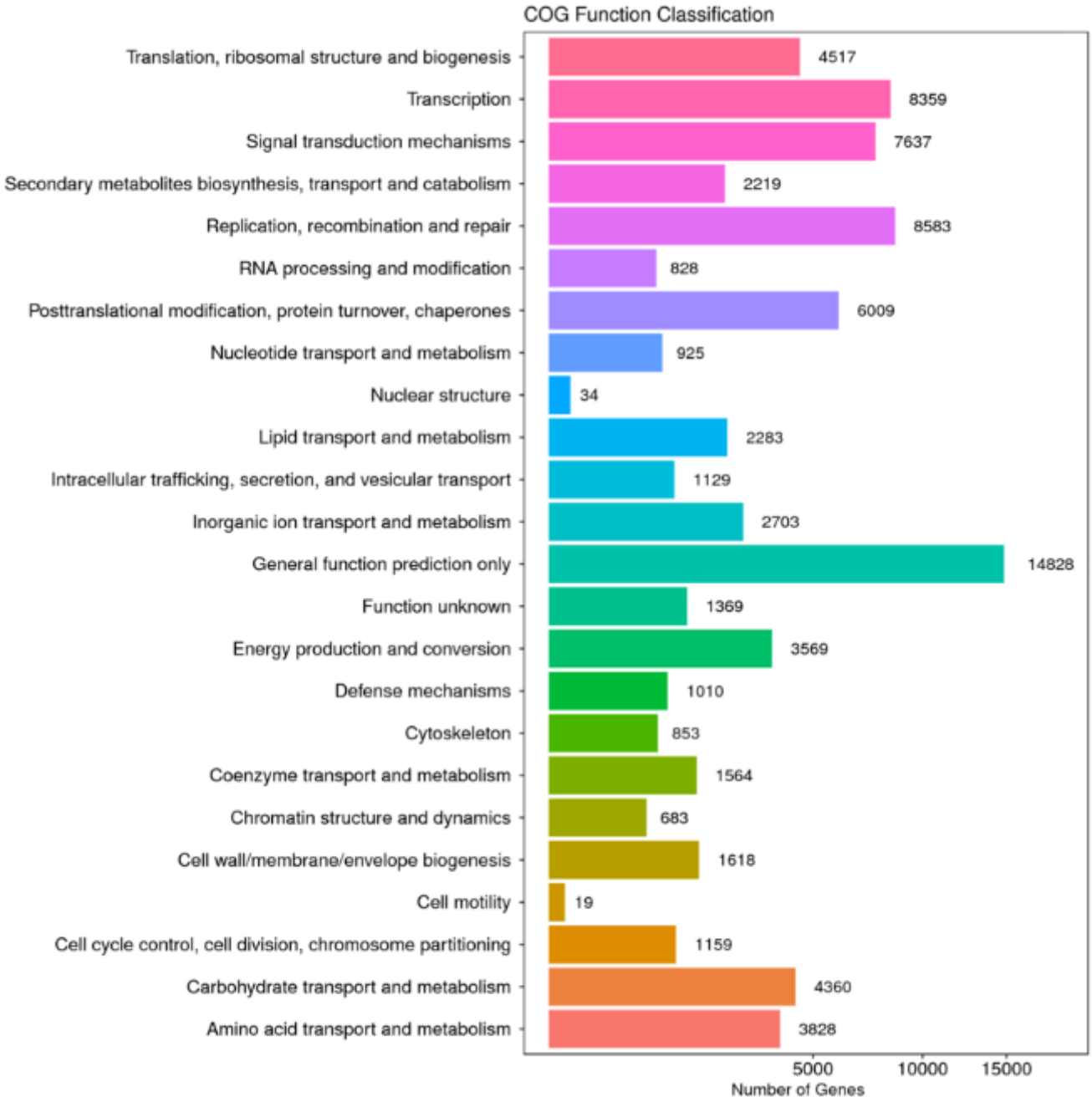

Figure 5

Unigene functions classified by cluster of orthologous groups (COG)

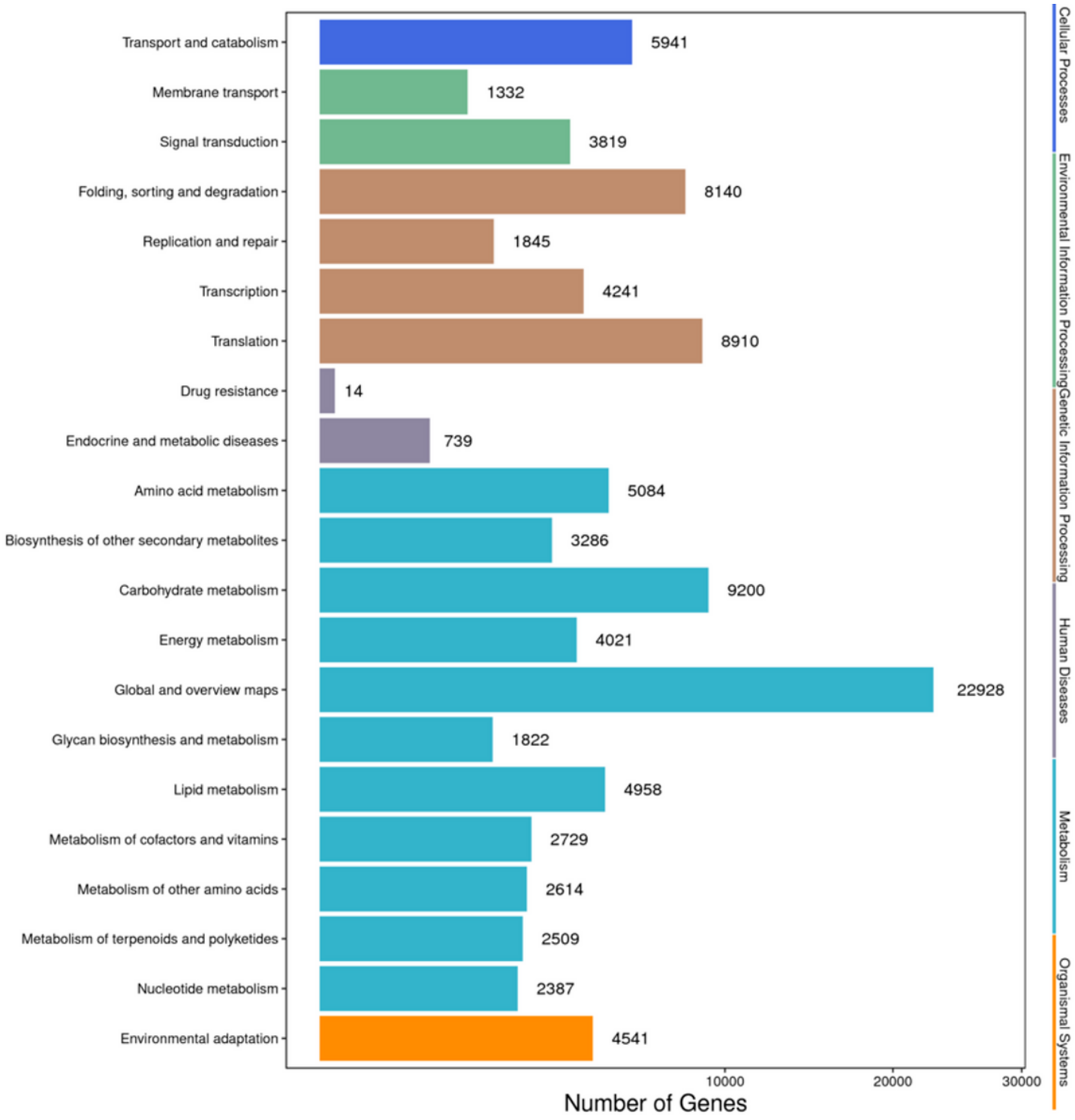

Figure 6

Pathway assignment based on the KEGG database

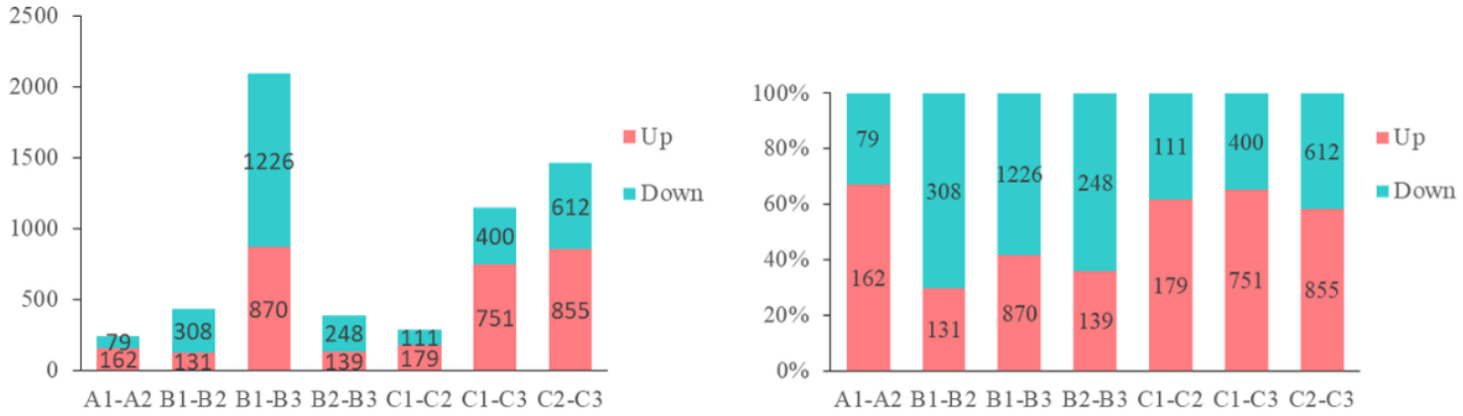

Figure 7

Numbers of differentially expressed genes (DEGs) between different individuals

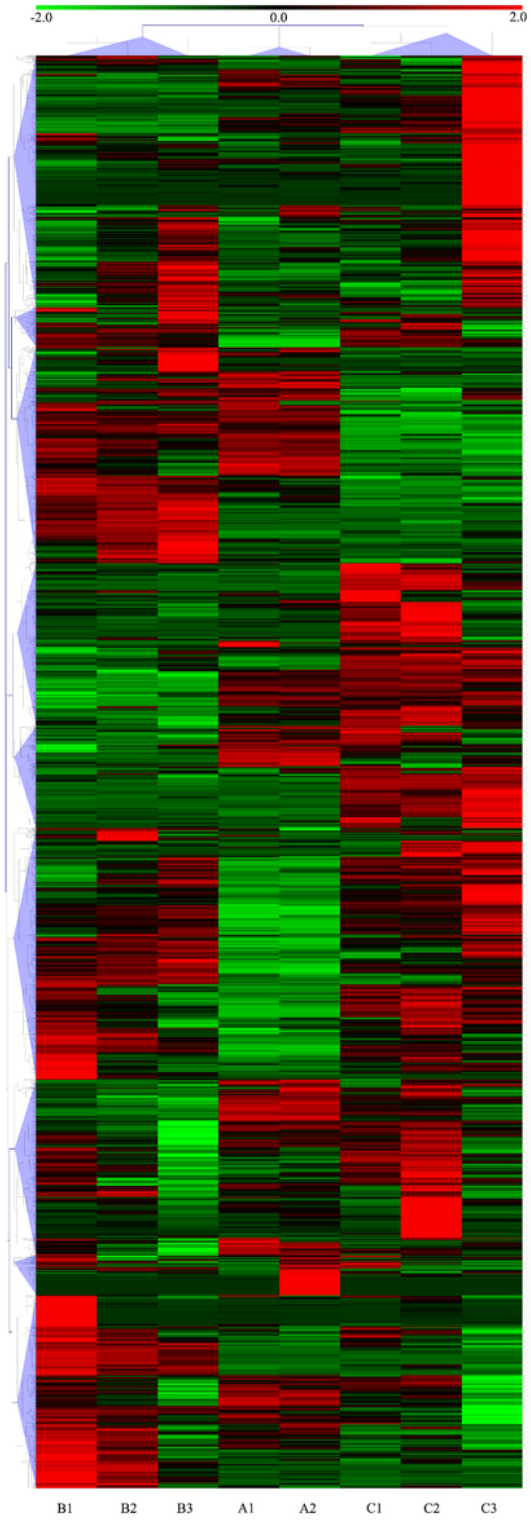

Figure 8

Hierarchical clustering of differentially expressed genes (DEGs) in different individuals

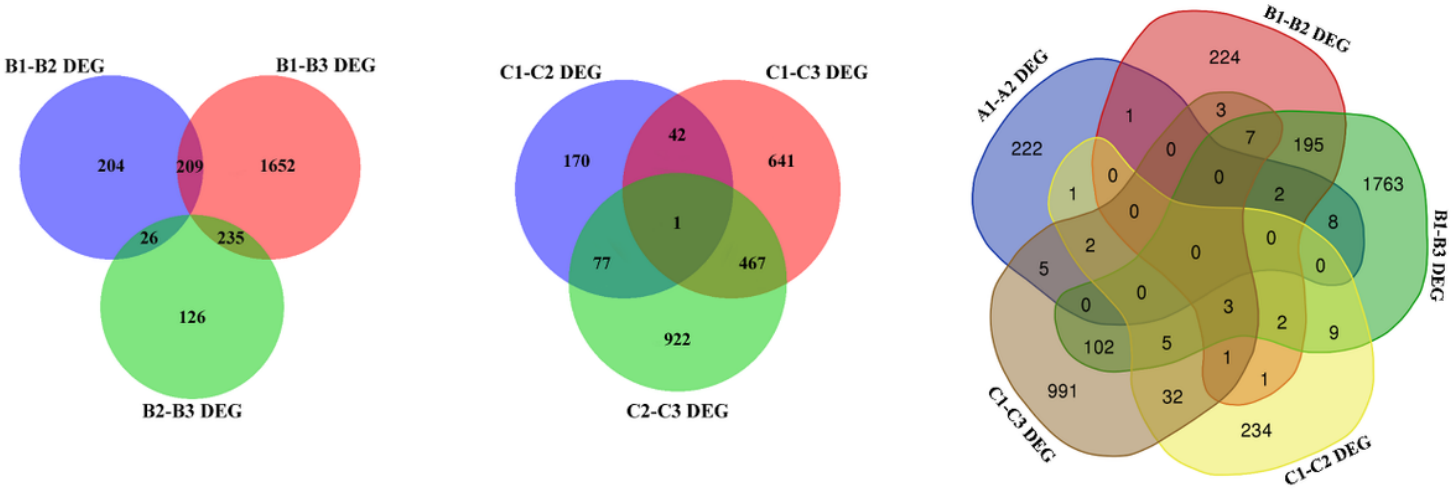

Figure 9

Venn diagram representation of DEGs from pairwise comparisons

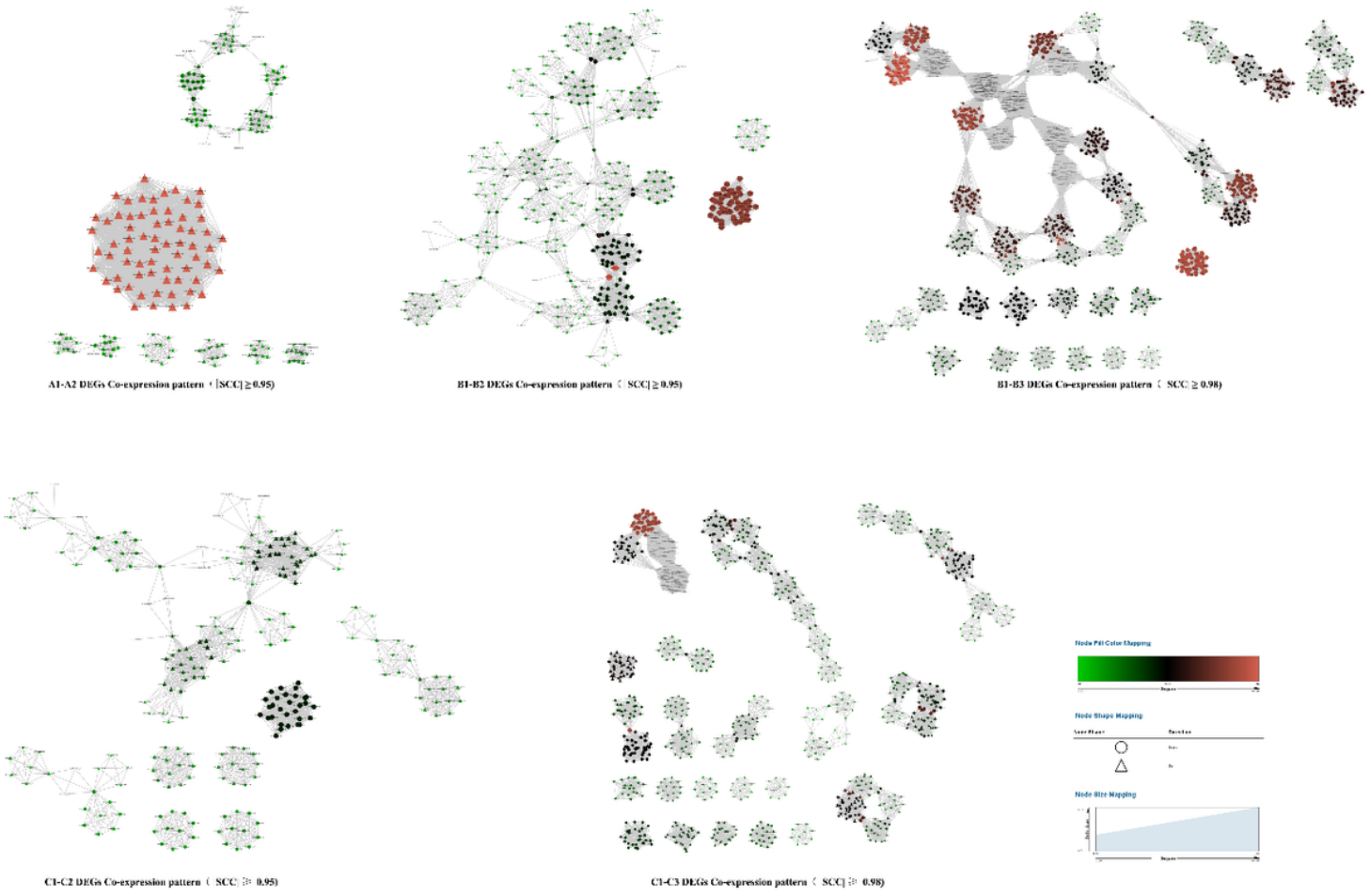

Figure 10

Co-expression network of differentially expressed genes (DEGs)

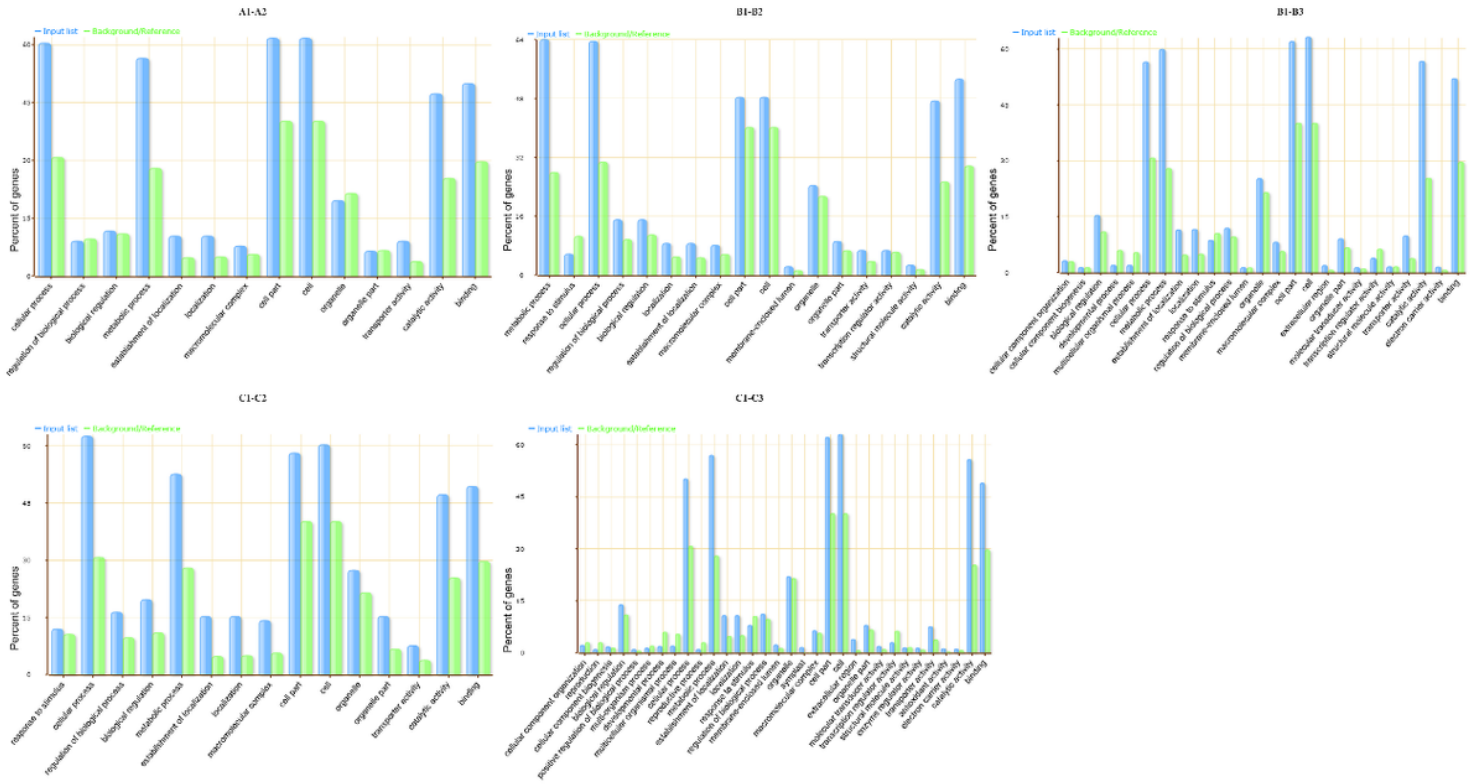

Figure 11

Differentially expressed genes (DEGs) gene ontology (GO) annotation

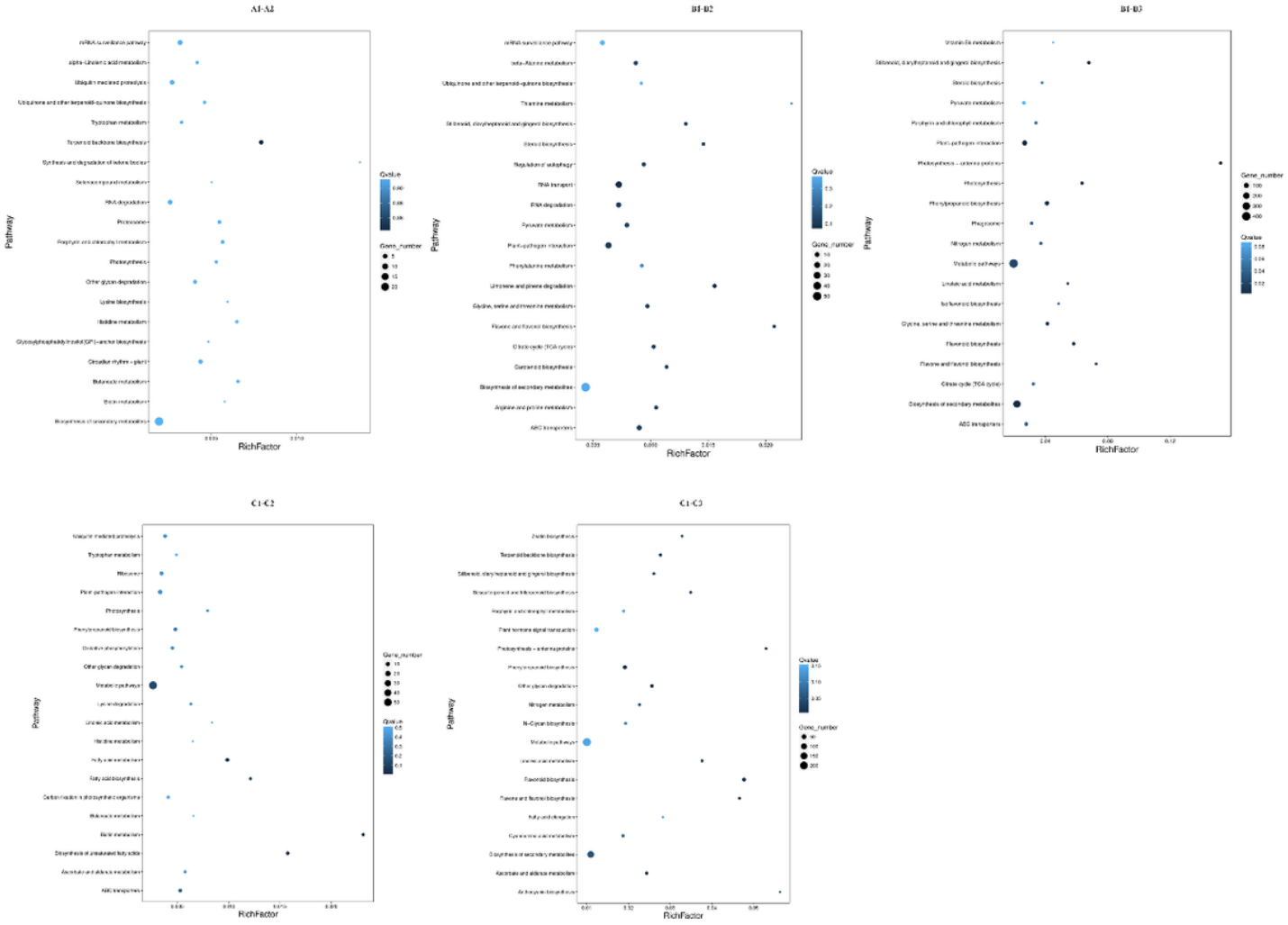

Figure 12

KEGG enrichment of differentially expressed genes (DEGs)

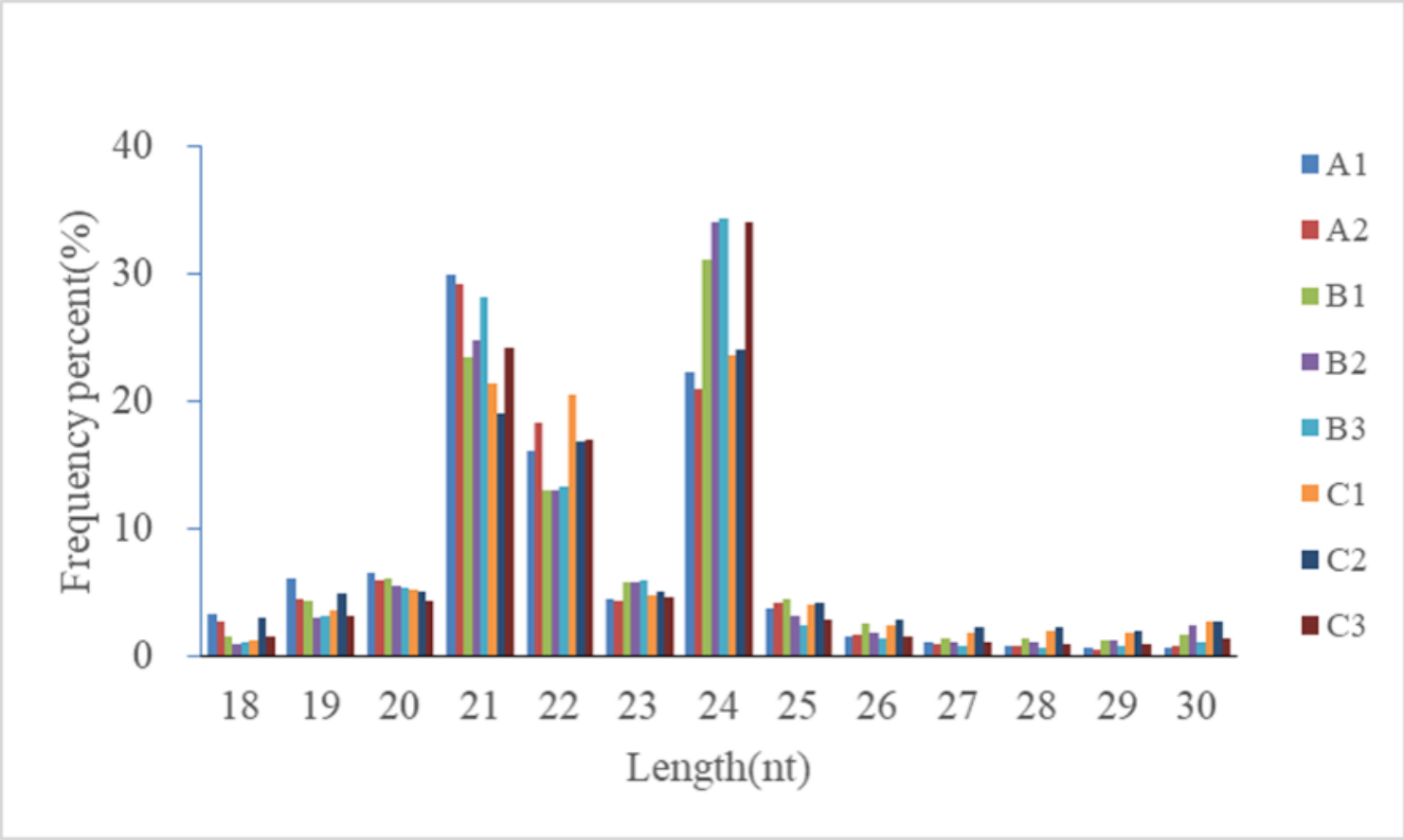

Figure 13

Length distributions of small RNAs

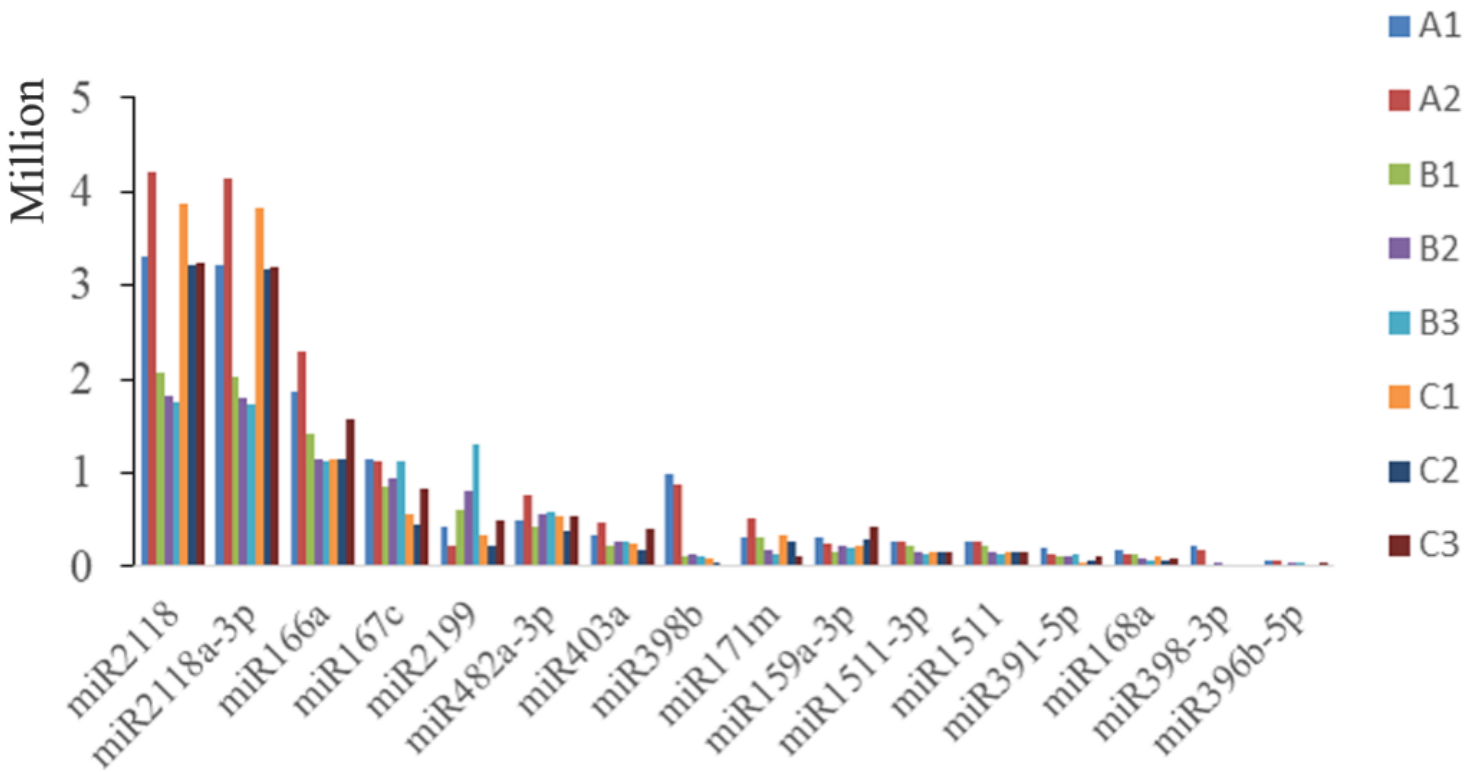

Figure 14

Most abundantly expressed known miRNAs involved in rejuvenation

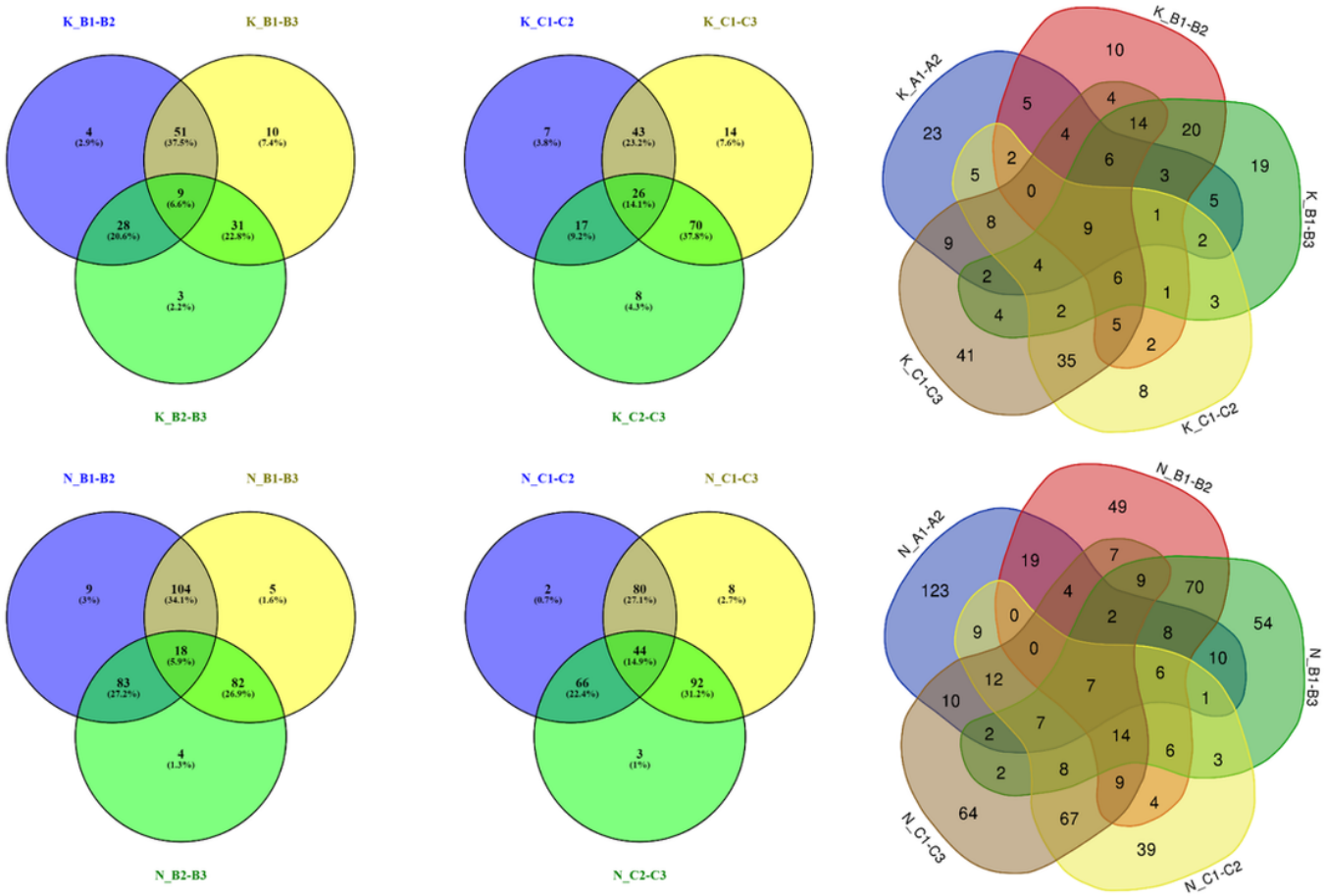

Figure 15

Venn diagram representation of differentially expressed miRNAs from pairwise comparisons. The beginning of K represents the known miRNAs; The beginning of N represents the novel miRNAs.

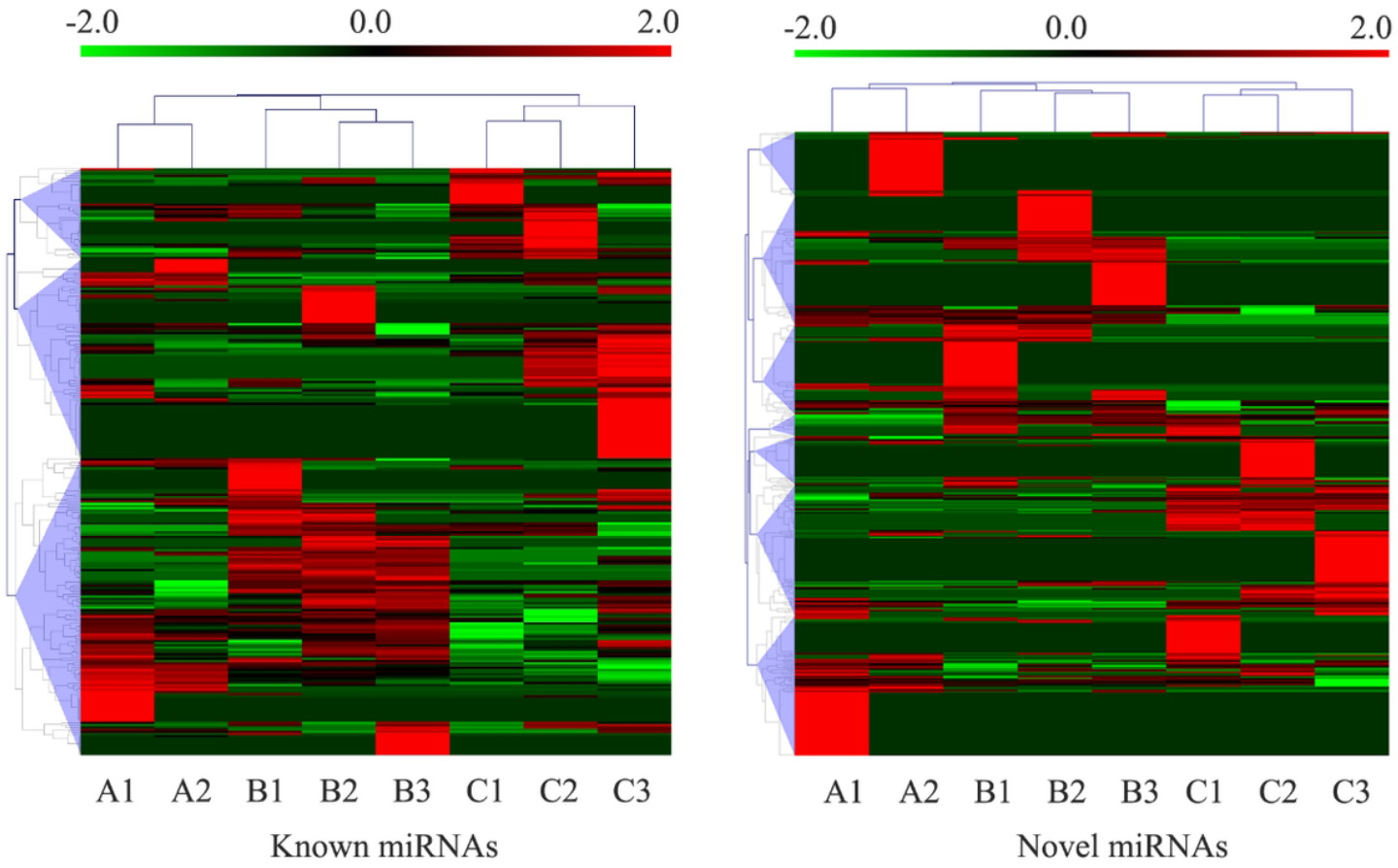

Figure 16

Hierarchical clustering of differentially expressed microRNAs

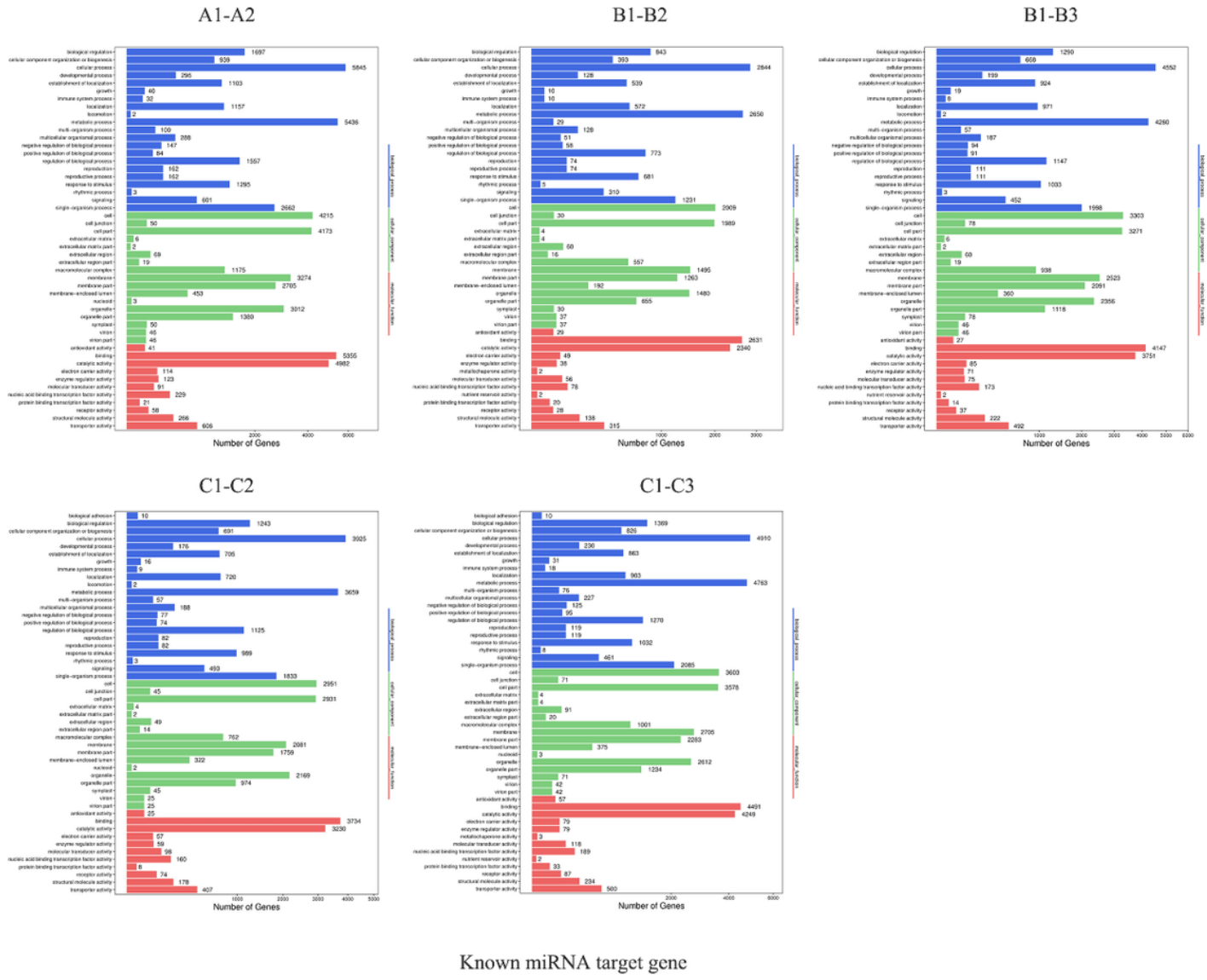

Figure 17

Gene ontology (GO) analysis of known miRNA target genes

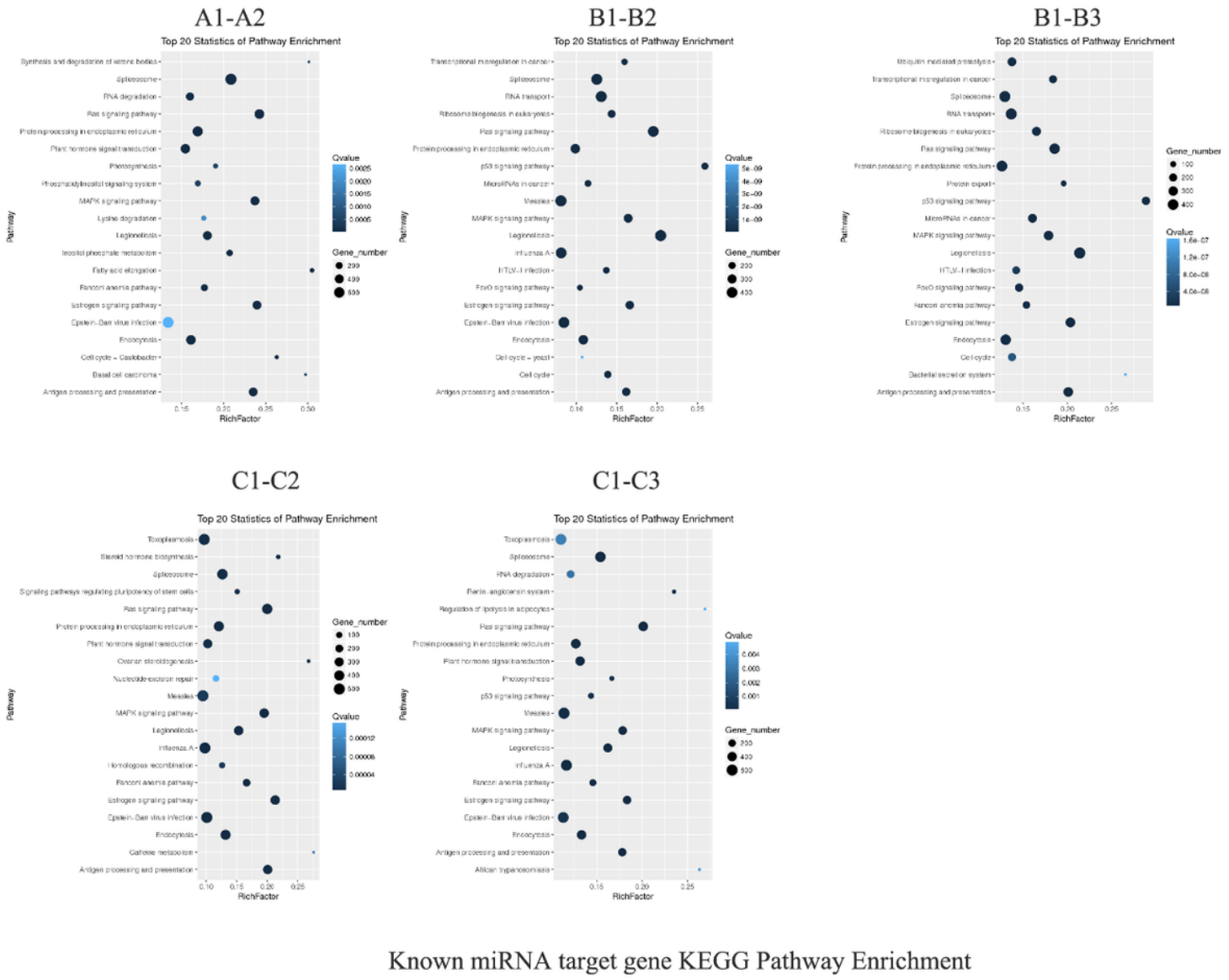

Figure 18

KEGG enrichment of known miRNA target genes

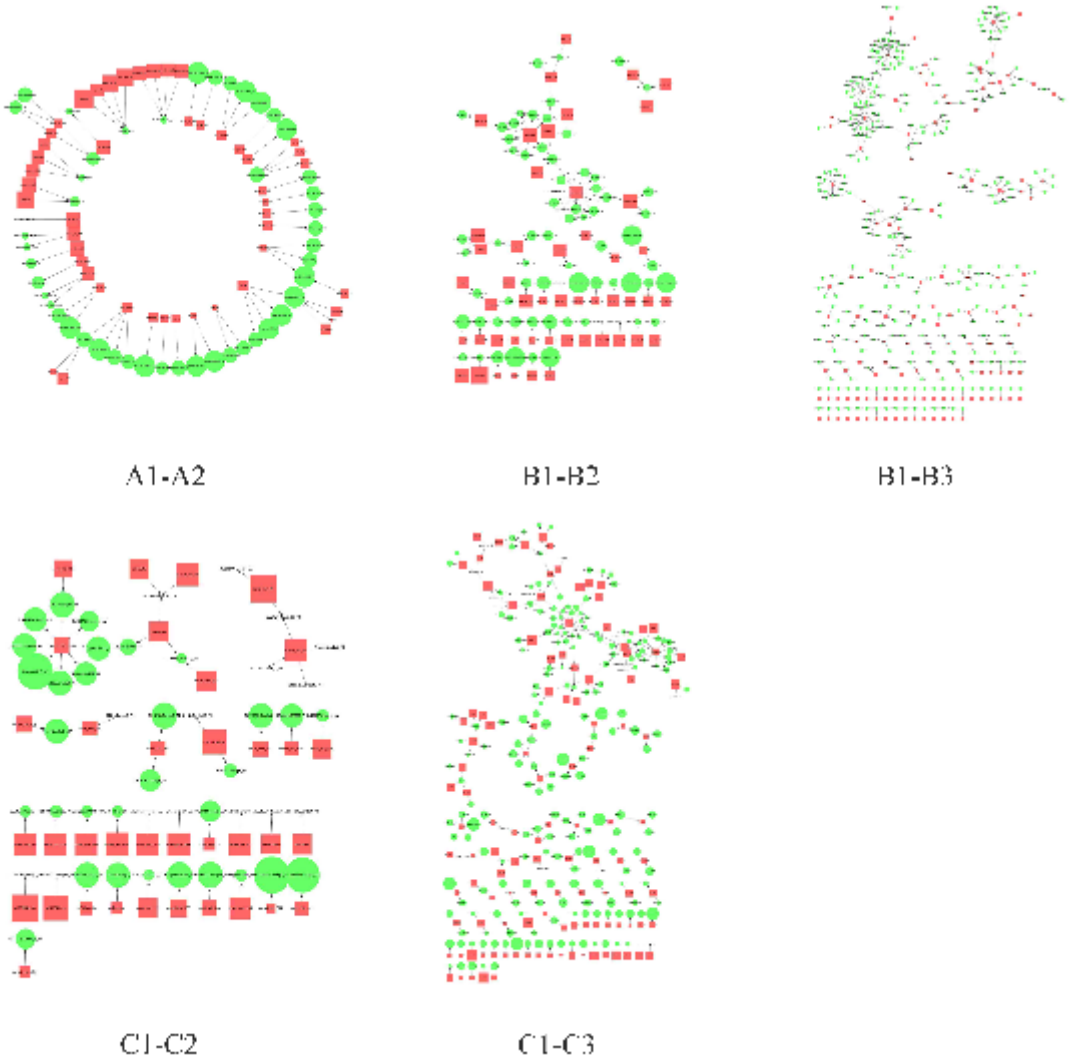

Figure 19

Network of putative interactions between miRNAs and mRNAs during rejuvenation. The red squares represent microRNAs and the green circles represent target genes predicted by RNA-seq analysis

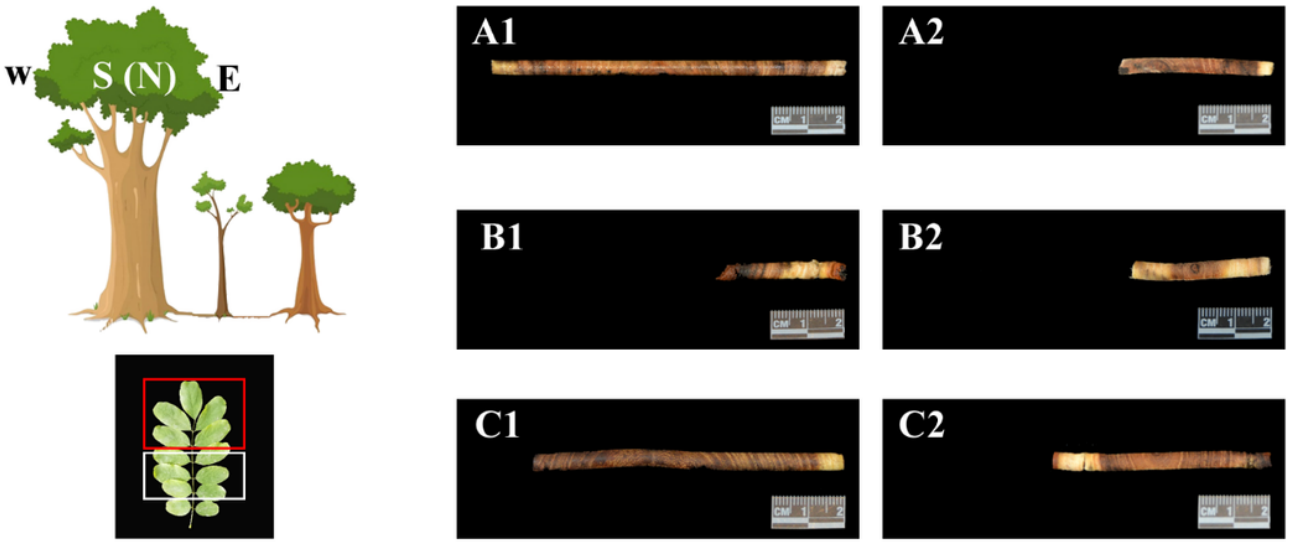

Figure 20

Schematic diagram of experimental materials. The upper left is the sampling site. The right is the wood core of each group. The lower left is the high-throughput sequencing material, the leaves in the red box were used for mRNA-Seq, and the leaves in the white box were used for miRNA-Seq.

Supplementary Files

This is a list of supplementary files associated with this preprint. Click to download.

- FigureS1.tif
- TableS1.xlsx
- TableS2.xlsx
- TableS3.xlsx
- TableS6.xlsx
- TableS5.xlsx
- FigureS3.tif
- TableS4.xlsx
- FigureS2.tif
- TableS7.xlsx
- TableS9.xlsx

- TableS8.xlsx